

AD-A184 813

# VIRGINIA TECH CENTER FOR ADHESION SCIENCE

VPI-E-87-9  
CAS/ESM-87-2

August 1987

BENDING OF A BONDED BEAM AS A TEST METHOD  
FOR ADHESIVE PROPERTIES

E. Moussiaux, Research Assistant  
Engineering Science and Mechanics

H. F. Brinson, Professor  
Engineering Science and Mechanics

A. H. Cardon, Professor  
Free University of Brussels

DTIC  
ELECTE  
SEP 18 1987  
S D

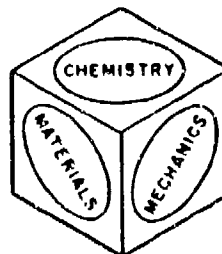
**DISTRIBUTION STATEMENT A**  
Approved for public release  
Distribution Unlimited

Support for this work was provided by the Office of Naval  
Research (Contract No. N00014-82-K-0185 P00005)  
Dr. Larry Peebles, Jr., Project Monitor  
Code 431  
800 N. Quincy Street  
Arlington, VA 22217

VIRGINIA POLYTECHNIC INSTITUTE  
AND STATE UNIVERSITY

216 NORRIS HALL  
BLACKSBURG, VIRGINIA 24061

Telephone: (703) 961-6824  
TLX: EZLINK 9103331861  
VPI-BKS



ADA184813

SECURITY CLASSIFICATION OF THIS PAGE

REPORT DOCUMENTATION PAGE

1a. REPORT SECURITY CLASSIFICATION Unclassified		7b. RESTRICTIVE MARKINGS	
2a. SECURITY CLASSIFICATION AUTHORITY		3. DISTRIBUTION/AVAILABILITY OF REPORT	
2b. DECLASSIFICATION/DOWNGRADING SCHEDULE			
4. PERFORMING ORGANIZATION REPORT NUMBER(S) VPI-E-87-9 CAS/ESM-87-2		5. MONITORING ORGANIZATION REPORT NUMBER(S)	
6a. NAME OF PERFORMING ORGANIZATION Virginia Polytechnic Institute & State University	6b. OFFICE SYMBOL (if applicable)	7a. NAME OF MONITORING ORGANIZATION	
6c. ADDRESS (City, State, and ZIP Code) Center for Adhesion Science 216 Norris Hall Blacksburg, VA 24061		7b. ADDRESS (City, State, and ZIP Code)	
8a. NAME OF FUNDING/SPONSORING ORGANIZATION Office of Naval Research	8b. OFFICE SYMBOL (if applicable)	9. PROCUREMENT INSTRUMENT IDENTIFICATION NUMBER	
8c. ADDRESS (City, State, and ZIP Code) Code 431 800 N. Quincy Street Arlington, VA 22217		10. SOURCE OF FUNDING NUMBERS	
		PROGRAM ELEMENT NO.	PROJECT NO.
		TASK NO.	WORK UNIT ACCESSION NO.
11. TITLE (Include Security Classification) BENDING OF A BONDED BEAM AS A TEST METHOD FOR ADHESIVE PROPERTIES			
12. PERSONAL AUTHOR(S) E. Moussiaux, H. F. Brinson, A. H. Cardon			
13a. TYPE OF REPORT	13b. TIME COVERED FROM Sept 86 TO June 87	14. DATE OF REPORT (Year, Month, Day) August 1987	15. PAGE COUNT 82
16. SUPPLEMENTARY NOTATION			
17. COSATI CODES		18. SUBJECT TERMS (Continue on reverse if necessary and identify by block number)	
FIELD	GROUP	SUB-GROUP	
19. ABSTRACT (Continue on reverse if necessary and identify by block number)			
<p>A strength-of-materials type solution is obtained for the shear stress state in the adhesive layer of a bonded cantilever beam subjected to an end load.</p> <p>The shear stress is constant through the thickness of the adhesive layer and varies from zero at the fixed end to a maximum value at the free end. This maximum value can, under certain conditions, be calculated from knowledge of the load and the beam geometry only. The adhesive's shear modulus can then be determined from a measurement of the shear strain in the adhesive layer.</p> <p>An expression for the beam deflection is also obtained. It contains a coefficient of adhesion which is potentially useful in evaluating surface treatments or other factors leading to different states of adhesion.</p> <p>Fracture mechanics application of the specimen, and nonlinear and viscoelastic adhesive behavior are briefly mentioned.</p>			
20. DISTRIBUTION/AVAILABILITY OF ABSTRACT <input checked="" type="checkbox"/> UNCLASSIFIED/UNLIMITED <input type="checkbox"/> SAME AS RPT. <input type="checkbox"/> DTIC USERS		21. ABSTRACT SECURITY CLASSIFICATION	
22a. NAME OF RESPONSIBLE INDIVIDUAL		22b. TELEPHONE (Include Area Code)	22c. OFFICE SYMBOL

# BENDING OF A BONDED BEAM AS A TEST METHOD FOR ADHESIVE PROPERTIES

**Abstract**

A strength-of-materials type solution is obtained for the shear stress state in the adhesive layer of a bonded cantilever beam subjected to an end load.

The shear stress is constant through the thickness of the adhesive layer and varies from zero at the fixed end to a maximum value at the free end. This maximum value can, under certain conditions, be calculated from knowledge of the load and the beam geometry only. The adhesive's shear modulus can then be determined from a measurement of the shear strain in the adhesive layer.

An expression for the beam deflection is also obtained. It contains a coefficient of adhesion which is potentially useful in evaluating surface treatments or other factors leading to different states of adhesion.

Fracture mechanics application of the specimen, nonlinear and viscoelastic adhesive behavior are briefly mentioned.



Accession For	
NTIS CRA&I	<input checked="" type="checkbox"/>
DTIC TAB	<input type="checkbox"/>
Unannounced	<input type="checkbox"/>
Justification .....	
By .....	
Distribution / .....	
Availability Codes	
Dist	Avail and/or Special
A-1	

## ACKNOWLEDGMENTS

The authors acknowledge with gratitude the source of funding for this work. The financial support was provided by the Office of Naval Research (ONR) N000 14-82-K-0185, Arlington, VA 22217; the project monitor was Dr. L. H. Peebles.

Thanks are given to Prof. G. Moussiaux and S. Roy for their valuable help through different stages of this work.

## Table of Contents

<b>1.0 INTRODUCTION</b> .....	<b>1</b>
<b>2.0 STRESSES AND DISPLACEMENTS IN AN ADHESIVELY BONDED CANTILEVER BEAM SUBJECTED TO AN END LOAD</b> .....	<b>5</b>
2.1 Introduction .....	5
2.2 Geometry and Notations .....	7
2.3 Shear Stress Distribution in the Adhesive Layer .....	8
2.3.1 Deflection and Continuity Equations .....	8
2.3.2 Differential Equation for the Shear Stress .....	14
2.3.3 Shear Stress Distribution .....	15
2.3.4 Limit Cases .....	17
2.3.5 Discussion of the Shear Stress in the Adhesive Layer .....	19
2.3.6 Experimental Aspects .....	25
2.4 Deflection of the Bonded Cantilever Beam .....	27
2.4.1 Integration of the Deflection Equation .....	27
2.4.2 Analysis of the End Deflection Expression .....	31
2.4.3 Experimental Aspects .....	34
2.5 Conclusions .....	38
<b>3.0 STRESS-FUNCTION SOLUTION</b> .....	<b>40</b>
3.1 Introduction .....	40
3.2 Stress State in the Beam .....	42
3.2.1 Stress Function Analysis (13) .....	42
3.2.2 Choice of the Stress Function Considering the Basic Assumptions .....	45

3.2.3	Boundary Conditions	47
3.2.4	Shear Stress in the Adhesive Layer	55
3.3	Deflection of the Cantilever	56
3.4	Comparison of the Two Solutions	56
3.5	Conclusions	60
<b>4.0</b>	<b>NUMERICAL EVALUATION OF THE STRENGTH OF MATERIALS SOLUTION</b>	<b>61</b>
4.1	Introduction	61
4.2	Shear Stress in the Adhesive Layer (Table 2)	63
4.3	Effect of the Loading Mode	67
4.4	Deflection of the Beam	69
4.5	Conclusions	72
<b>5.0</b>	<b>RECOMMENDATIONS FOR FUTURE WORK</b>	<b>74</b>
5.1	Introduction	74
5.2	Nonlinear Adhesive Behavior	74
5.3	Viscoelastic Material Behavior	76
5.4	Fracture Mechanics Application	78
5.5	Conclusions	80
<b>6.0</b>	<b>CONCLUSIONS</b>	<b>81</b>
<b>7.0</b>	<b>References</b>	<b>82</b>

## List of Illustrations

Figure 1.	Short beam shear test for composites. ....	2
Figure 2.	Three-point bending of a bonded beam. ....	4
Figure 3.	Three-point bending - cantilever beam analogy. ....	6
Figure 4.	Geometry of the cantilever beam. ....	7
Figure 5.	Cantilever beam cut along the midplane of the adhesive layer. ....	8
Figure 6.	Relative displacement due to bending. ....	10
Figure 7.	Relative displacement due to shear deformation of the adhesive. ....	11
Figure 8.	Normal deformation of a beam in tension. ....	12
Figure 9.	Relative displacement due to normal deformation of the adherends. ....	13
Figure 10.	Parameter ....	20
Figure 11.	Shear stress in an isotropic cantilever beam subjected to an end load. ....	21
Figure 12.	Shear stress variation in the adhesive layer along the length of the beam. ....	22
Figure 13.	Maximum shear stress in the adhesive layer as a function of adhesive deformability. ....	24
Figure 14.	Maximum shear strain in the adhesive layer as a function of adhesive deformability. ....	26
Figure 15.	Dependence of the end deflection of the cantilever on the adhesive deformability for various $t/h$ . ....	32
Figure 16.	Dependence of the end deflection of the cantilever on the adhesive deformability for various $l/h$ . ....	33
Figure 17.	Dependence of the dimensions of a test beam on the absolute value of the thickness of the adhesive layer (scale 1/1). ....	36
Figure 18.	Graphical solution for $G_a$ from a deflection measurement ....	37
Figure 19.	Coefficient of adhesion $\beta$ ....	38
Figure 20.	Definition of $h$ for both methods. ....	41
Figure 21.	Geometry of the bonded beam for the stress function solution. ....	42

Figure 22. Stresses in a two-dimensional problem. ....	43
Figure 23. Deformation of an element of adhesive in the adhesive layer. ....	49
Figure 24. Comparison of the shear stress in the adhesive for the two solutions. ....	58
Figure 25. Comparison of the end deflection of the beam for both solutions. ....	59
Figure 26. Discretization of the beam. ....	61
Figure 27. Comparison of numerically and theoretically obtained shear stress. ....	64
Figure 28. Variation of shear stresses over the thickness of the adhesive layer for various positions along the x-axis. ....	65
Figure 29. Comparison of numerically and theoretically obtained maximum shear stress values in the adhesive layer. ....	66
Figure 30. Effect of loading mode. ....	67
Figure 31. Shear stresses and normal vertical stresses in the adhesive layer for one-sided loading. ....	68
Figure 32. Comparison of the end deflection of the beam obtained by finite element analysis and by the strength-of-materials solution. ....	69
Figure 33. Comparison of the deflection of the cantilever beam obtained by finite elements and by the strength-of-materials solution. ....	70
Figure 34. Deflection of a steel-rubber beam, compared to the cases of "perfect adhesion" and "no adhesion" ....	71
Figure 35. Deflection of an aluminum-epoxy beam, compared to the cases of "perfect adhesion" and "no adhesion" ....	72
Figure 36. Creep loading. ....	78
Figure 37. Double cantilever beam test. ....	79
Figure 38. Bonded cantilever subjected to an end load. ....	79
Figure 39. Bonded cantilever beam in mixed mode loading. ....	80

## 1.0 INTRODUCTION

In the last decade, adhesives have increasingly been used in structural bonds, especially in high-performance sectors like the aeronautical industry. Advantages of adhesive bonding are manifold: fatigue behavior of adhesively bonded joints is better than for the traditional bolted, welded, or riveted joints; loads are more uniformly transferred from one adherend to the other; there is no local weakening of the adherends due to bolt holes; weight of the actual bonding area is reduced; joint surfaces are smoother; etc. However, there are disadvantages, and at least two major problems arise when adhesives are used to bond structural parts. First, the stress state is usually complex and not accurately known; and, second, environmental effects can seriously alter joint performance to the extent that long-term integrity is not predictable.

Numerical techniques, mostly finite element analyses, give good understanding of the first problem, providing material properties are known. Because of the variety of material properties, as well as the effect of environment on properties, a great variety of test geometries and test specimens has resulted. The reason there is no single generally accepted test is that each has its shortcomings in various degrees. Some are reasonably well analyzed but require costly machining and fabrication while others are simple to make but give only average or over-simplified moduli. Moreover, many adhesives exhibit complex material characteristics such as nonlinear and/or time-dependent behavior. In addition, the chemical or mechanical bonding between adherends and adhesives is not well understood. The interface or interphase layer between adherend and adhesive is not well defined, especially in regard to the measurement of mechanical properties. There is also some question as to whether the properties of the bulk adhesive differ from those of the thin film of adhesive in an actual joint.

The Short Beam Shear Test (SBST) is an ASTM Standard Test (1), used to obtain the interlaminar shear strength of composite materials (1-11). In this test a short composite beam is loaded to failure in three-point bending (Figure 1). Span-to-thickness ratios may vary from 4 to 7 depending on the fiber type in the composite (1). In elastic beam theory, the maximum shear stress, at the midplane, in three-point bending is given by equation [1.1], in which  $b$  is the width of the beam.

$$\tau_{\max} = \frac{3P}{4bh} \quad [1.1]$$

At failure,  $P = P_f$ , the interlaminar shear strength  $S_{II}$  is then given by

$$S_{II} = \frac{3P_f}{4bh} \quad [1.2]$$

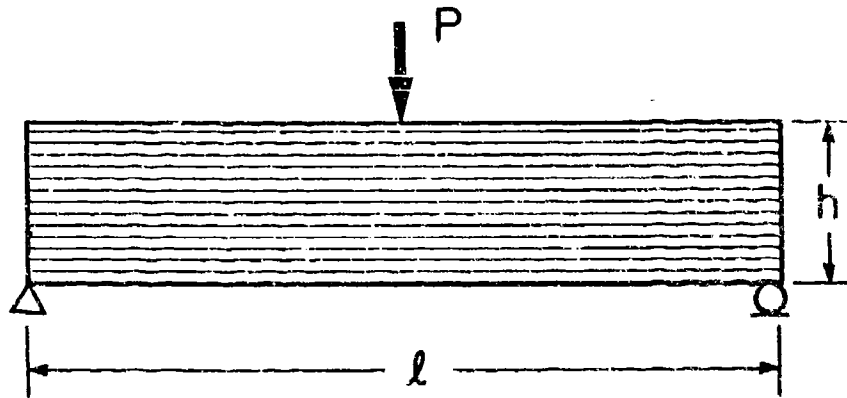


Figure 1. Short beam shear test for composites.

Because the beam is short, Saint-Venant effects cannot be neglected as they are in the elastic beam theory leading to expression [1.1], which assumes a constant shear state. Thus the interlaminar shear strength, as obtained in the SBST, will only be an "apparent" interlaminar shear strength. Therefore ASTM advises that this value be used only for quality control and not for design (1).

Whitney and Browning (2,3) raised another point of caution about the SBST, stating that very often fiber buckling in the neighborhood of the load leads to failure at the midsurface prior to that predicted by theory. Browning, Abrams and Whitney (4) proposed to replace the SBST by a test using four-point bending that, in their experiments, routinely produced the desired interlaminar shear failure mode.

Stinchcomb, Henneke and Price (5) went even further and completely rejected the SBST for quality control of advanced composites. They observed experimentally that for graphite-polyimide laminates, only those which were poorly manufactured failed in shear.

Notwithstanding the above objections to the SBST for composites, the question arose as to whether such a simple test geometry of a beam in three-point-bending, or a cantilever beam loaded at the end, could be used to measure the shear properties of an adhesive layer bonded to two adherends (Figure 2). To obtain properties it is necessary to calculate or know *a priori* the stress state at a material point and to relate this known stress to measurable shear deformation in the adhesive layer, or even easier, at the midpoint deflection of the beam. It is the purpose of this study to obtain a closed-form analytical solution to a beam composed of two adherends bonded together with an adhesive. The finite element method will also be used to obtain a numerical solution. The two solutions will be compared. The intent is to provide a basis for the measurement of shear properties with this technique. As a result, optimum features of geometry and properties of adherends and adhesives will be identified to maximize achieving accurate measurements.

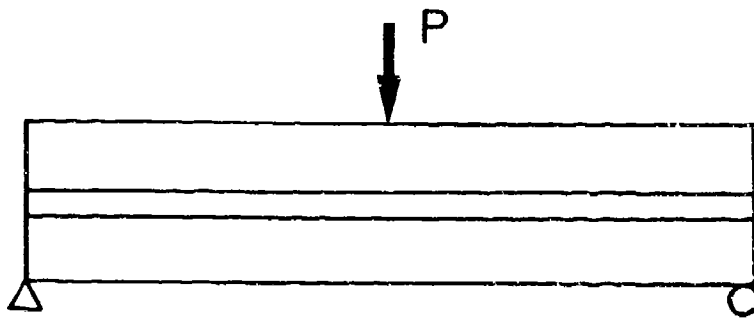


Figure 2. Three-point bending of a bonded beam.

---

## 2.0 STRESSES AND DISPLACEMENTS IN AN ADHESIVELY BONDED CANTILEVER BEAM SUBJECTED TO AN END LOAD

### 2.1 Introduction

In this chapter a solution will be presented for the state of stress and for the displacements in an adhesively bonded cantilever beam subjected to an endload. More particularly, the shear stress distribution along the length of the adhesive layer will be examined. Also, the experimental use of this test geometry will be extensively discussed.

The idea of the method of analysis is to subject the cantilever beam to an endload and to cut the adhesive layer along its midplane, thus freeing the shear stresses in this layer. Expressing continuity of displacements along both sides of the cut, together with the deflection equations for the adherends, will result in a differential equation in the unknown shear stress. This equation will eventually be solved using the proper boundary conditions.

A similar method was first used in 1962 by Hubert Beck (12), in an article in which the author examined the shear forces in connecting floors between two shear walls of a high-rise building.

Three basic assumptions are made in the present analysis:

- the adhesive layer is in a state of pure shear.
- the adherends obey the Euler-Bernoulli beam theory.
- both adhesive and adherends are linear elastic.

The validity of the first assumption will depend upon the thickness and stiffness of the adhesive layer and how the load is transferred to the beam. This last point will be discussed in a later section. For thick and stiff adhesive layers, normal stresses are likely to develop as they do in a monolithic beam. A consequence of the second assumption is that the adherends may not be "short beams,"

which is, in fact, an ill-defined term. Usually a beam is called "short" when its length-to-thickness ratio is less than ten.

The solution will be valid for both a beam in three-point bending and a cantilever beam subjected to an endload, assuming the latter to be perfectly clamped. Due to symmetry, the midsection of the beam in three-point-bending will undergo no rotation, nor will the fixed end of the cantilever beam. If the load on the cantilever beam equals the support reactions of the three-point-bending beam, then the vertical displacement of the midsection of the single beam will be equal to the end deflection of the cantilever (Figure 3).

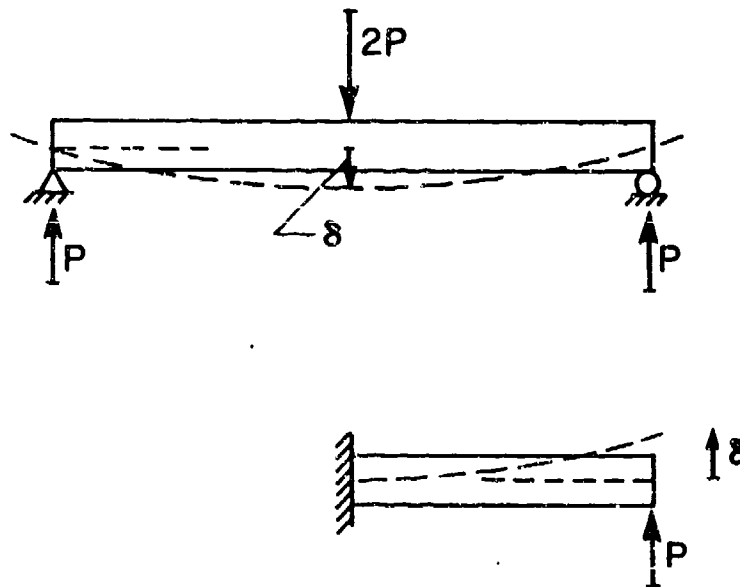


Figure 3. Three-point bending - cantilever beam analogy.

---

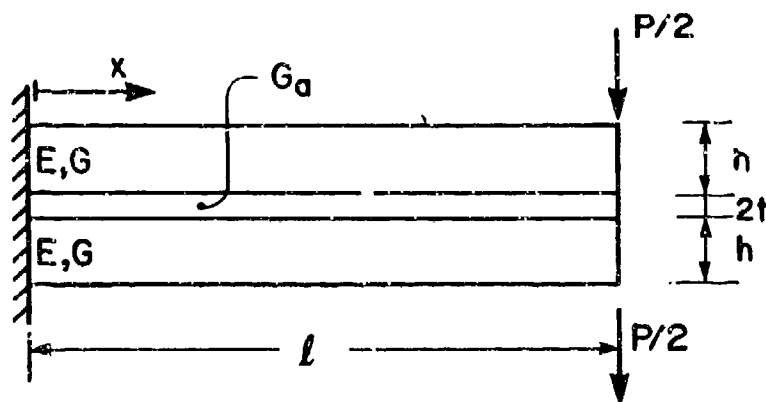


Figure 4. Geometry of the cantilever beam.

## 2.2 Geometry and Notations

The following symbols will be used in the remainder of this chapter (Figure 4). The cantilever beam is symmetrical with respect to its midplane.

Geometry	Material Properties
$l$ : length of the cantilever	$E$ : Young's modulus of the adherends
$h$ : thickness of an adherend	$G$ : shear modulus of the adherends
$t$ : half the thickness of the adhesive layer	$G_a$ : shear modulus of the adhesive
$b$ : width of the beam	

The vertical deflection  $v$  is chosen positive for downward motion. Transverse deformations due to Poisson effects are neglected.

To complete the symmetry and to avoid compressive stresses in the adhesive layer, half of the load  $P$  is applied to the upper adherend, half to the lower adherend.

## 2.3 Shear Stress Distribution in the Adhesive Layer

### 2.3.1 Deflection and Continuity Equations

The adhesive layer of the loaded beam is cut along its midplane (Figure 5). On both sides of the cut, the unknown shear stress in the adhesive layer,  $\tau_{xy}(x)$ , is then exposed. The direction of the shear stress will be so that it counteracts the relative motion of the surfaces along the cut, due to the bending of the adherends caused by their end loads.

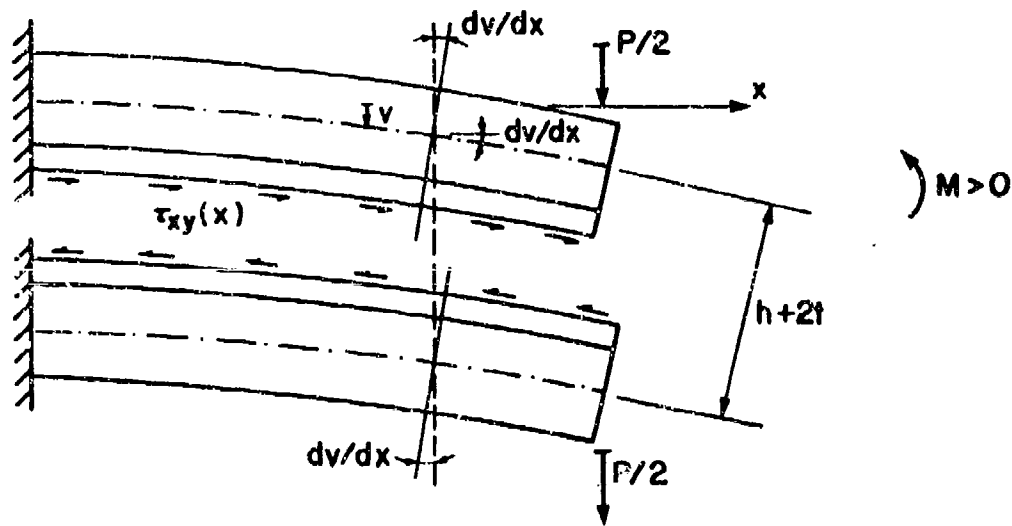


Figure 5. Cantilever beam cut along the midplane of the adhesive layer.

In the assumption that Euler-Bernoulli beam theory is valid for the adherends, the deflection equation for the upper adherend is given by:

$$\frac{d^2v}{dx^2} = -\frac{M}{EI} \quad [2.1]$$

in which  $v$  is the deflection of the adherend,  $M$  is the applied moment on the adherend with respect to its midplane, and  $I$  is the moment of inertia of the adherend, again with respect to the midplane.

$$I = \frac{bh^3}{12} \quad [2.2]$$

M is taken to be positive when the lowest fiber of the adherend is stretched.

The applied moment has a negative component due to the applied load  $P/2$  and a positive component due to the unknown shear stress  $\tau_{xy}$  acting at a distance  $h/2 + t$  away from the midplane of the adherend.

$$M(x) = -\frac{P}{2}(\ell - x) + b\left(\frac{h}{2} + t\right) \int_x^\ell \tau_{xy}(\eta) d\eta \quad [2.3]$$

Combining equations [2.1] and [2.3] results in the deflection equation:

$$EI \frac{d^2v}{dx^2} = \frac{P}{2}(\ell - x) - b \frac{h + 2t}{2} \int_x^\ell \tau_{xy}(\eta) d\eta \quad [2.4]$$

If no shear stress acted along the exposed adhesive surface, two neighboring points on each side of the cut (Figure 5) would move apart due to the individual bending deformations of both adherends. It is to prevent this motion that shear stresses must exist in the adhesive layer.

To assure continuity, it is then necessary that the total relative displacement, due to internal and external loads, of those two originally neighboring points be set at zero. This relative displacement has three distinct components: one due to bending of the adherends, the second due to shear deformation of the adhesive layer, and the third due to normal deformation of the adherends caused by the integrated shear stress. Only the horizontal components will be considered.

The relative displacement component due to bending of the adherends,  $\delta_1(x)$ , can be readily obtained from Figure 6 and is arbitrarily taken positive.

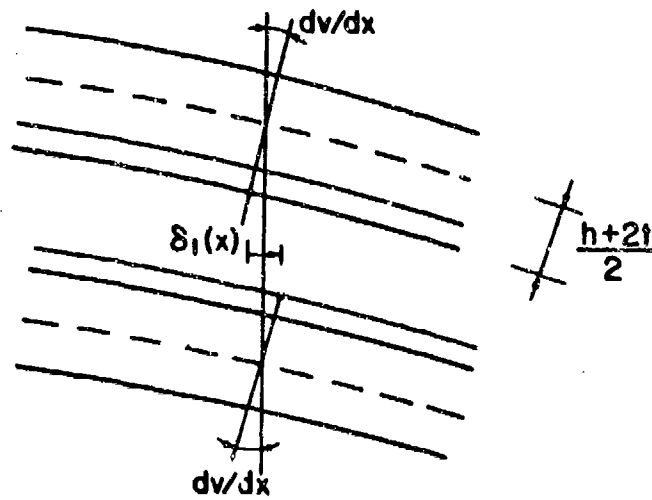


Figure 6. Relative displacement due to bending.

$$\delta_1(x) = 2 \cdot \frac{h+2t}{2} \cdot \frac{dv}{dx} = (h+2t) \frac{dv}{dx} \quad [2.5]$$

The relative displacement component due to shear deformation of the adhesive,  $\delta_2(x)$ , is determined from Figure 7.

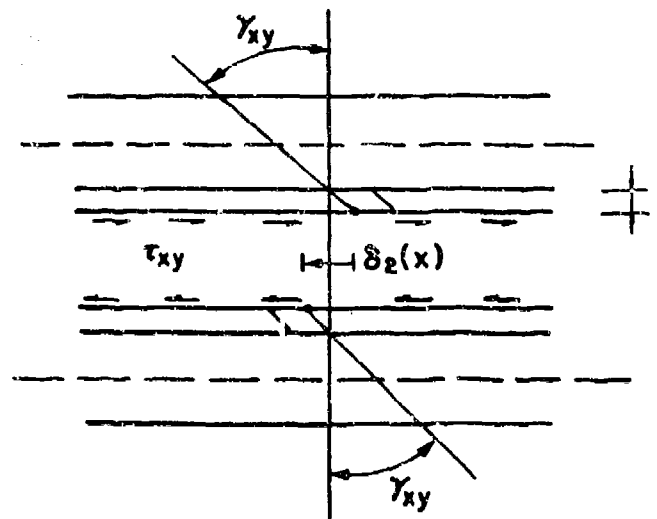


Figure 7. Relative displacement due to shear deformation of the adhesive.

$$\delta_2(x) = -2t\gamma_{xy}(x) = -2t\frac{\tau_{xy}(x)}{G_a} \quad [2.6]$$

Because the relative displacement of each point is in the opposite direction to the bending component,  $\delta_2(x)$  must be negative. The minus sign is necessary because  $\delta_2(x)$  is negative and  $\tau_{xy}$  is taken positive as shown. The adhesive is assumed to be linear elastic to obtain equation [2.6].

In addition to contributing to bending stresses in the adherends, the shear stress in the adhesive layer will induce a net axial force in both adherends, tensile in the upper and compressive in the lower. These normal forces will cause a third displacement component for points along the exposed middle surface of the adhesive.

In a beam loaded by normal stresses only, the displacements are found by integrating the normal strains (Figure 8),

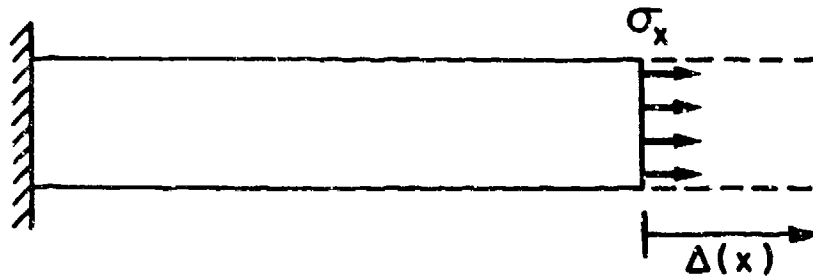


Figure 8. Normal deformation of a beam in tension.

$$\Delta(x) = \int_0^x \varepsilon_x(\eta) d\eta = \int_0^x \frac{\sigma_x(\eta)}{E} d\eta \quad [2.7]$$

This normal stress,  $\sigma_x(\eta)$ , in the bonded cantilever is the total force obtained by integration of the shear stresses from point  $\eta$  to the end of the beam, divided by the transversal area of the adherend,

$$\sigma_x(\eta) = \frac{1}{bh} \int_{\eta}^{\ell} b \tau_{xy}(\lambda) d\lambda \quad [2.8]$$

Substitution of equation [2.8] into equation [2.7] leads to,

$$\Delta(x) = \int_0^x \int_{\eta}^{\ell} \frac{\tau_{xy}(\lambda)}{Eh} d\lambda d\eta \quad [2.9]$$

The relative displacement component of the two points along the adhesive surface,  $\delta_3(x)$ , is then obtained from Figure 9. Like the second component,  $\delta_3(x)$  is negative also.

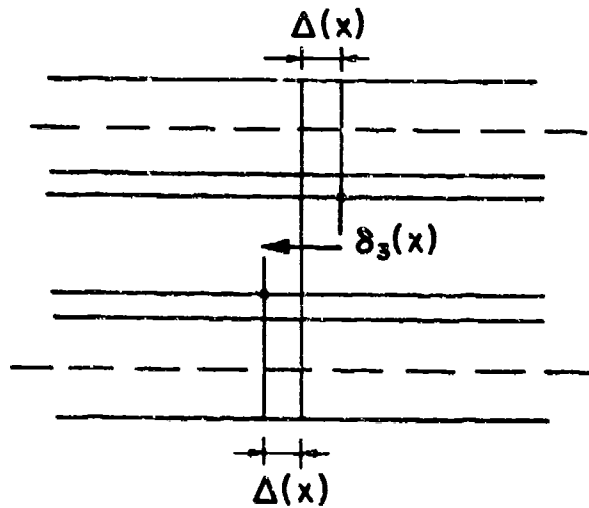


Figure 9. Relative displacement due to normal deformation of the adherends.

$$\delta_3(x) = -\frac{2}{Eh} \int_0^x \int_{\eta}^{\ell} \tau_{xy}(\lambda) d\lambda d\eta \quad [2.10]$$

The continuity equation finally is,

$$\delta_1(x) + \delta_2(x) + \delta_3(x) = 0 \quad [2.11]$$

or,

$$(h + 2t) \frac{dv}{dx} - 2t \frac{\tau_{xy}}{G_a} - \frac{2}{Eh} \int_0^x \int_{\eta}^{\ell} \tau_{xy}(\lambda) d\lambda d\eta = 0 \quad [2.12]$$

In the next section the deflection equation [2.6] and the continuity equation [2.12] will be combined and will lead to a differential equation in the unknown shear stress  $\tau_{xy}(x)$ .

### 2.3.2 Differential Equation for the Shear Stress

In the previous section, the basic equations governing the shear stress state in the beam were developed. These equations need now to be combined and integrated to lead to the actual shear stress distribution in the adhesive layer.

First, the continuity equation is to be differentiated twice with respect to  $x$ . Some theorems concerning integral calculus have to be used to take the derivative of the integral term. These are,

$$\frac{d}{dx} \int_a^x f(\eta) d\eta = f(x) \quad [2.13a]$$

and

$$\int_x^a f(\eta) d\eta = - \int_a^x f(\eta) d\eta \quad [2.13b]$$

Taking the first derivative of equation [2.12] leads to,

$$(h + 2t) \frac{d^2 v}{dx^2} - \frac{2t}{G_a} \frac{d\tau_{xy}}{dx} - \frac{2}{Eh} \int_x^{\ell} \tau_{xy}(\lambda) d\lambda = 0 \quad [2.14]$$

and taking the second derivative, to,

$$(h + 2t) \frac{d^3 v}{dx^3} - \frac{2t}{G_a} \frac{d^2 \tau_{xy}}{dx^2} + \frac{2}{Eh} \tau_{xy}(x) = 0 \quad [2.15]$$

Differentiating the deflection equation [2.4] once with respect to  $x$  gives,

$$EI \frac{d^3 v}{dx^3} = - \frac{P}{2} + b \left[ \frac{h + 2t}{2} \right] \tau_{xy}(x) \quad [2.16]$$

Elimination of the deflection term from equations [2.15] and [2.16], and some rearrangement, leads to the differential equation in the unknown shear stress,

$$\frac{d^2 \tau_{xy}}{dx^2} - \left[ \frac{G_a b}{4EI} (h + 2t)^2 + \frac{G_a}{Eth} \right] \tau_{xy} = - \frac{G_a (h + 2t)}{4tEI} P \quad [2.17]$$

Introducing  $t/h$  as a dimensionless adhesive thickness and  $\ell/h$  as a slenderness ratio and using the expression for the inertia moment  $I$ , equation [2.17] can be rewritten as,

$$\begin{aligned} \frac{d^2 \tau_{xy}}{dx^2} - 3 \frac{G_a}{E} \left[ \frac{\ell}{h} \right]^2 \frac{(1 + 2t/h)^2}{t/h} \frac{1}{\ell^2} \left[ 1 + \frac{1}{3(1 + 2t/h)^2} \right] \tau_{xy} \\ = - \frac{P}{b(h + 2t)\ell^2} 3 \frac{G_a}{E} \left[ \frac{\ell}{h} \right]^2 \frac{(1 + 2t/h)^2}{t/h} \end{aligned} \quad [2.18]$$

Now the following parameters are defined,

$$\alpha^2 = 3 \frac{G_a}{E} \left[ \frac{\ell}{h} \right]^2 \frac{(1 + 2t/h)^2}{t/h} \quad [2.19]$$

$$\gamma^2 = 1 + \frac{1}{3(1 + 2t/h)^2} \quad [2.20]$$

$$\bar{\alpha} = \alpha \gamma \quad [2.21]$$

Substitution of these in equation [2.18] results in,

$$\frac{d^2 \tau_{xy}}{dx^2} - \left[ \frac{\bar{\alpha}}{\ell} \right]^2 \tau_{xy} = - \frac{P}{b(h + 2t)} \left[ \frac{\bar{\alpha}}{\gamma \ell} \right]^2 \quad [2.22]$$

To obtain the final form of the second order differential equation,  $x$  is replaced by a dimensionless coordinate  $\xi$ .

$$\xi = \frac{x}{\ell} \quad [2.23]$$

$$\frac{d^2 \tau_{xy}(\xi)}{d\xi^2} - \bar{\alpha}^2 \tau_{xy}(\xi) = - \frac{P}{b(h + 2t)} \left[ \frac{\bar{\alpha}}{\gamma} \right]^2 \quad [2.24]$$

### 2.3.3 Shear Stress Distribution

The general solution of a second order differential equation with constant coefficients, consists of a homogeneous part and a particular part.

$$\tau_{xy} = \tau_{xy}^h + \tau_{xy}^p \quad [2.25]$$

By inspection, the particular solution can be found to be,

$$\tau_{xy}^p = \frac{P}{b\gamma^2(h + 2t)} \quad [2.26]$$

The homogeneous solution for an equation of form [2.24] is,

$$\tau_{xy}^h = c_1 \cosh \bar{\alpha}\xi + c_2 \sinh \bar{\alpha}\xi \quad [2.27]$$

The complete solution is given by,

$$\tau_{xy} = \frac{P}{b\gamma^2(h + 2t)} + c_1 \cosh \bar{\alpha}\xi + c_2 \sinh \bar{\alpha}\xi \quad [2.28]$$

in which the integration constants  $C_1$  and  $C_2$  are to be found using the boundary conditions. At the fixed end, for  $\xi = 0$  and  $x = 0$ ,

$$\frac{dv}{dx} = 0 \quad [2.29]$$

Setting  $dv/dx$  equal to zero in the continuity equation [2.12] and considering that an integral with equal integration limits vanishes, leads to,

$$\tau_{xy}(\xi = 0) = 0 \quad [2.30]$$

and

$$c_1 = \frac{-P}{b\gamma^2(h + 2t)} \quad [2.31]$$

At the loaded end, the applied moment, and thus the curvature, is zero.

$$\begin{array}{l} \text{For } x = l \\ \xi = 1 \end{array} : \frac{d^2v}{dx^2} = -\frac{M}{EI} = 0 \quad [2.32]$$

Taking the derivative of the continuity equation [2.12] and evaluating the resulting equation for  $x = l$  leads to:

$$\left. \frac{d\tau_{xy}}{dx} \right|_{x=\ell} = 0 \quad [2.32a]$$

or,

$$\left. \frac{d\tau_{xy}}{d\xi} \right|_{\xi=1} = 0 \quad [2.32b]$$

and,

$$c_1 \bar{\alpha} \sinh \bar{\alpha} + c_2 \bar{\alpha} \cosh \bar{\alpha} = 0 \quad [2.32c]$$

so that,

$$c_2 = \frac{P \tanh \bar{\alpha}}{b\gamma^2(h + 2t)} \quad [2.33]$$

Finally, expression [2.34] is obtained for the shear stress distribution in the adhesive layer,

$$\tau_{xy} = \frac{P}{b\gamma^2(h + 2t)} (1 - \cosh \bar{\alpha}\xi + \tanh \bar{\alpha} \sinh \bar{\alpha}\xi) \quad [2.34]$$

Stresses and displacements in the adherends can be computed using Euler-Bernoulli beam theory for a cantilever loaded by a shear stress as given in [2.34] and a cantilever loaded by an end load  $P/2$ .

#### 2.3.4 Limit Cases

In this section the two limit cases of "perfect adhesion" and "no adhesion" will be investigated.

Perfect adhesion is assumed to be obtained when the bonded beam behaves like a monolithic beam with no adhesive layer. This condition is met when the thickness of the adhesive layer approaches zero. Therefore the limits for vanishing  $t$  have to be examined for  $\alpha$ ,  $\gamma$ ,  $\bar{\alpha}$  and  $\tau_{xy}$ .

The perfect adhesion case is not defined as the limit case for which the adhesive's shear modulus approaches the adherend's shear modulus, since this definition would violate the pure shear assumption in the adhesive layer.

$$\lim_{t \rightarrow 0} \alpha^2 = \lim_{t \rightarrow 0} \left\{ 3 \frac{G_a}{E} \left[ \frac{\ell}{h} \right]^2 \frac{(1 + 2t/h)^2}{t/h} \right\} = \infty \quad [2.35]$$

$$\lim_{t \rightarrow 0} \gamma^2 = \lim_{t \rightarrow 0} \left\{ 1 + \frac{1}{3(1 + 2t/h)^2} \right\} = \frac{4}{3} \quad [2.36]$$

$$\lim_{t \rightarrow 0} \bar{\alpha} = \lim_{t \rightarrow 0} [\alpha \gamma] = \infty \quad [2.37]$$

$$\begin{aligned} \lim_{t \rightarrow 0} \tau_{xy} &= \frac{3P}{4bh} \left( 1 - \cosh \infty + \frac{\sinh \infty}{\cosh \infty} \sinh \infty \right) \\ &= \frac{3P}{4bh} \left[ 1 - \frac{1}{\cosh \infty} (\cosh^2 \infty - \sinh^2 \infty) \right] \\ &= \frac{3P}{4bh} \left[ 1 - \frac{1}{\cosh \infty} \right] \\ &= \frac{3P}{4bh} \end{aligned} \quad [2.38]$$

This shear stress is exactly the maximum shear stress in a monolithic and homogeneous cantilever beam of thickness  $2h$ , subjected to an endload  $P$ .

For the case of "no adhesion," the adhesive has to be infinitely deformable, or, in other words, the adhesive's shear modulus  $G$  has to approach zero. Taking again the necessary limits, it is clear that the shear stress goes, logically, to zero in the "adhesive" layer.

$$\lim_{G_a \rightarrow 0} \bar{\alpha}^2 = \lim_{G_a \rightarrow 0} \left\{ \gamma^2 3 \frac{G_a}{E} \left[ \frac{\ell}{h} \right]^2 \frac{(1 + 2t/h)^2}{t/h} \right\} = 0 \quad [2.39]$$

$$\lim_{G_a \rightarrow 0} \tau_{xy} = \lim_{G_a \rightarrow 0} \left\{ \frac{P}{b\gamma^2(h + 2t)} (1 - \cosh 0 + \tanh 0 \cdot \sinh 0) \right\} = 0 \quad [2.40]$$

In the following the shear stress distribution will be analyzed for the whole range of adhesives between these limit cases.

### 2.3.5 Discussion of the Shear Stress in the Adhesive Layer

The variation of the shear stress in the adhesive layer along the length of the cantilever is given by equation [2.34],

$$\tau_{xy}(\xi) = \frac{P}{b\gamma^2(h+2t)}(1 - \cosh \bar{\alpha}\xi + \tanh \bar{\alpha} \cdot \sinh \bar{\alpha}\xi) \quad [2.34]$$

From this expression it's seen that the spatial dependence of the shear stress is governed by the parameter  $\bar{\alpha}$ , which is in turn related to  $\alpha$  and  $\gamma$ . To enhance the following discussion, equations on these quantities are repeated below,

$$\alpha^2 = 3 \frac{G_a}{E} \left[ \frac{\ell}{h} \right]^2 \frac{(1 + 2t/h)^2}{t/h} \quad [2.19]$$

$$\gamma^2 = 1 + \frac{1}{3(1 + 2t/h)^2} \quad [2.20]$$

$$\bar{\alpha} = \alpha\gamma \quad [2.21]$$

The quantity  $\bar{\alpha}$  contains all beam characteristics, both geometrical and material. Generally,  $\bar{\alpha}$  will increase with adhesive stiffness and beam length and decrease with adhesive thickness. The exact variation of  $\bar{\alpha}$  as a function of adhesive deformability,  $E/G_a$ , is given in Figure 10 for various adhesive thicknesses and slenderness ratios. For aluminum adherends bonded with an epoxy adhesive, for example,  $E/G_a$  will be somewhere between 100 and 1000, leading to values of  $\bar{\alpha}$  in the neighborhood of 10 or less for common geometries.

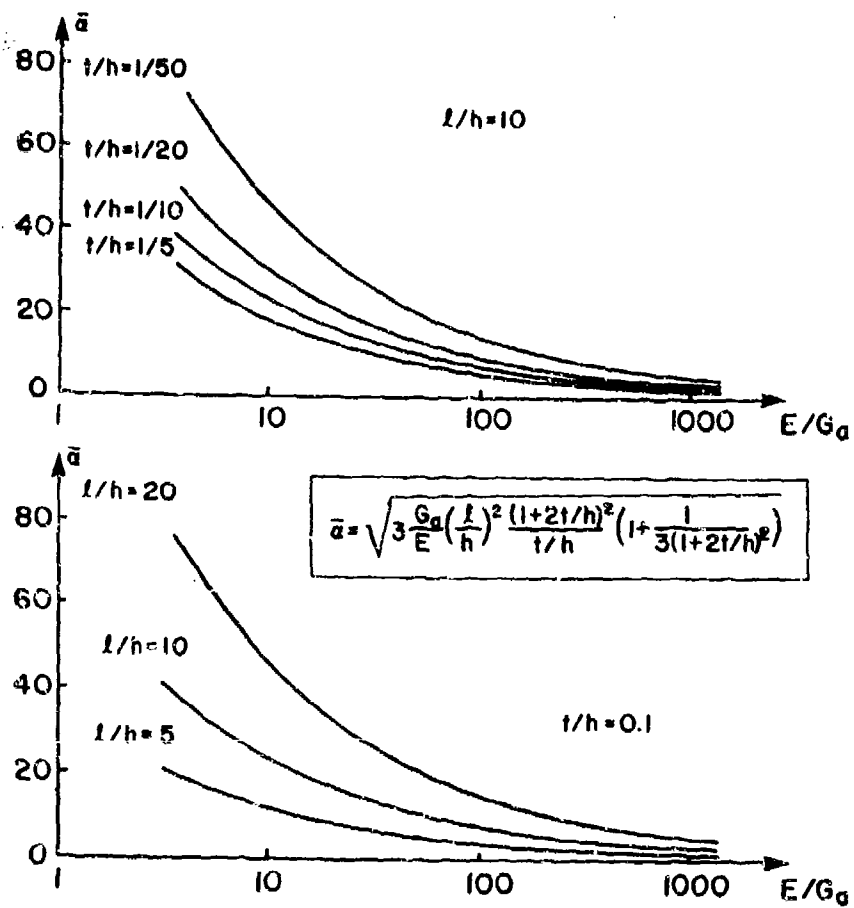


Figure 10. Parameter  $\bar{a}$ .

For a cantilever beam, loaded at the end by a force  $P$ , the external shear force diagram is constant, equalling  $P$ . In a monolithic homogeneous beam the shear stress state is directly related to the external shear force, resulting in a constant shear stress distribution along the length of the beam. From the elementary strength of materials, the variation over the thickness of the beam is known to be parabolic (Figure 11).

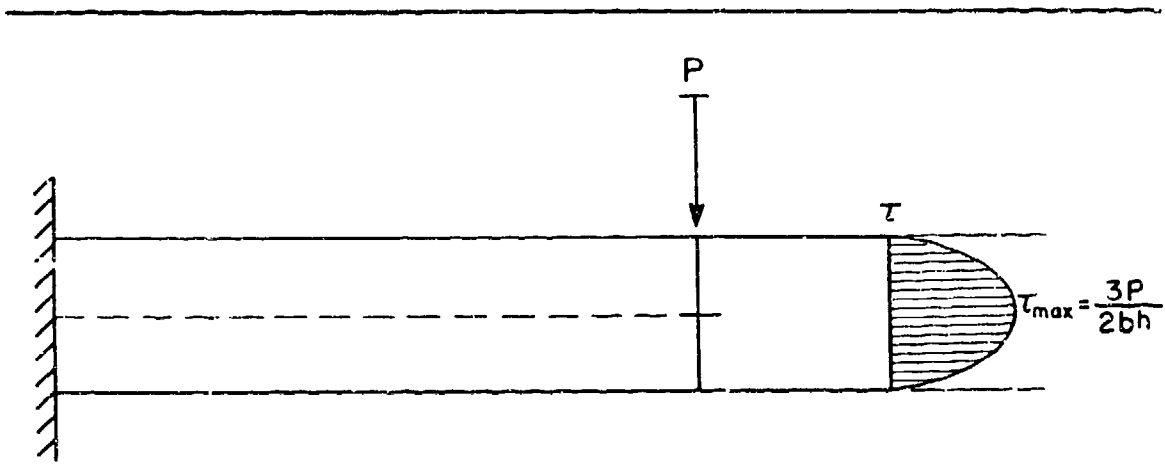


Figure 11. Shear stress in an isotropic cantilever beam subjected to an end load.

In a bonded cantilever beam, however, the shear stress in the adhesive is not directly related to the external shear force, but to the relative displacements of the adherends on each side of the adhesive layer. This relative motion of the adherends induces shear deformations in the adhesive layer and therefore also shear stresses. At the fixed end of the cantilever, although axial stresses and strains in the adherends are highest due to the maximum bending moment, there is no relative displacement between the adherends, because the displacement at the fixed support is zero. Thus, shear strains and shear stresses are zero in the adhesive layer at the fixed end. Further away from the clamped end, relative motion of the adherends begins to develop, thus building up shear stresses in the adhesive, until, in most cases, a stable value is reached.

This shear stress variation from the fixed end ( $\xi = 0$ ) to the free end ( $\xi = 1$ ) is shown in Figure 12, for various values of parameter  $\bar{\alpha}$ . It is seen in this figure that, for increasing  $\bar{\alpha}$ , more and more a constant shear state is approached as  $\bar{\alpha}$  is increased. A high  $\bar{\alpha}$  means a thin or stiff adhesive layer or a long beam. For low  $\bar{\alpha}$ , the shear stress varies along most of the length of the beam. A rough physical explanation for these facts is that it takes "longer" for the adherends to develop the relative displacements corresponding to a stabilized shear state as the adhesive layer gets thicker or more deformable.

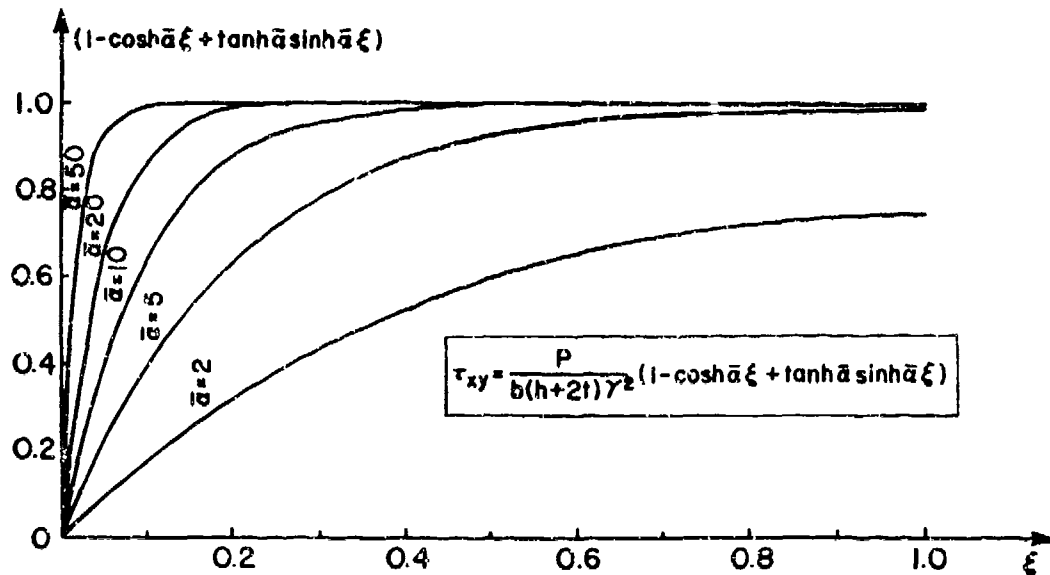


Figure 12. Shear stress variation in the adhesive layer along the length of the beam.

The maximum shear stress is always encountered at the free end of the cantilever. An expression for this maximum shear stress is obtained by setting  $\xi = 1$  in equation [2.34].

$$\tau_{xy}^{\max} = \frac{P}{b\gamma^2(h+2t)} \left( 1 - \cosh \bar{a} + \frac{\sinh \bar{a}}{\cosh \bar{a}} \sinh \bar{a} \right)$$

$$\tau_{xy}^{\max} = \frac{P}{b\gamma^2(h+2t)} \left[ 1 - \frac{1}{\cosh \bar{a}} \right] \quad [2.41]$$

In section 2.3.4, the limits for the shear stress in the cases of perfect adhesion and no adhesion were examined. Figure 13 shows how the maximum shear stress varies for a total range of geometries and adhesive properties. A logarithmic scale is used to allow a complete representation, from

very stiff to very deformable adhesives. Both graphs show three distinct zones. For very stiff adhesives, the maximum shear stress has a constant value, depending only on the thickness of the adhesive layer. The shear stress is a maximum in the zone of higher  $\bar{u}$  values, so that the second term in parentheses in equation [2.41] vanishes, leaving only the component dependent on the adhesive thickness. For very deformable adhesives, approaching the case of no adhesion, shear stresses drop to zero. The middle zone, approximately two decades wide, can be seen as an interaction zone, where both geometrical and adhesive properties are important.

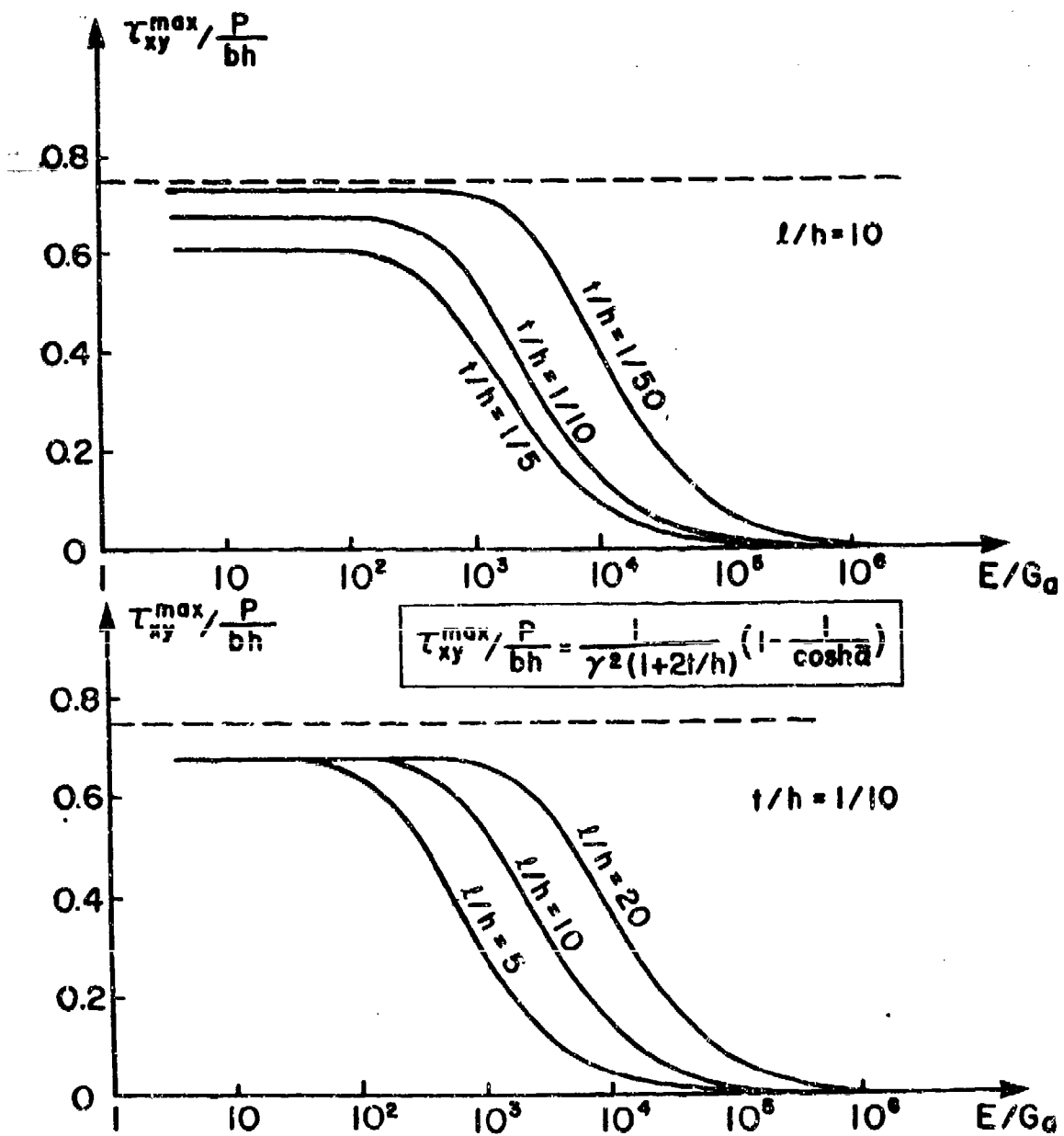


Figure 13. Maximum shear stress in the adhesive layer as a function of adhesive deformability.

A noteworthy feature of these curves is that they can be "shifted" by a mere change of geometrical parameters. For example, making the beam longer, or the adhesive layer thinner, will extend the constant shear zone.

### 2.3.6 Experimental Aspects

The constant maximum shear zone as discussed in the previous section is particularly interesting when it comes to using the bonded cantilever beam as a test device for measuring adhesive properties.

For this range of "stiffer" adhesives, it is possible to calculate the maximum shear stress in the adhesive layer from geometrical characteristics only. If a measurement of the shear strain in the adhesive can be obtained at the place of maximum stress, the shear modulus can be easily found, assuming linear elastic adhesive behavior. Such a measurement could, for example, be done by tracking the displacements of some points on each side of the adhesive layer using modern optical devices.

The maximum shear strain,  $\gamma_{xy}^{\max}$ , in the adhesive layer may be expressed as,

$$\gamma_{xy}^{\max} = \frac{\tau_{xy}^{\max}}{G_a} = \frac{P}{Ebh} \frac{E/G_a}{\gamma^2(1 + 2t/h)} \left[ 1 - \frac{1}{\cosh \bar{\alpha}} \right] \quad [2.42]$$

The maximum shear strain is represented graphically in Figure 14 as a function of geometry and properties.

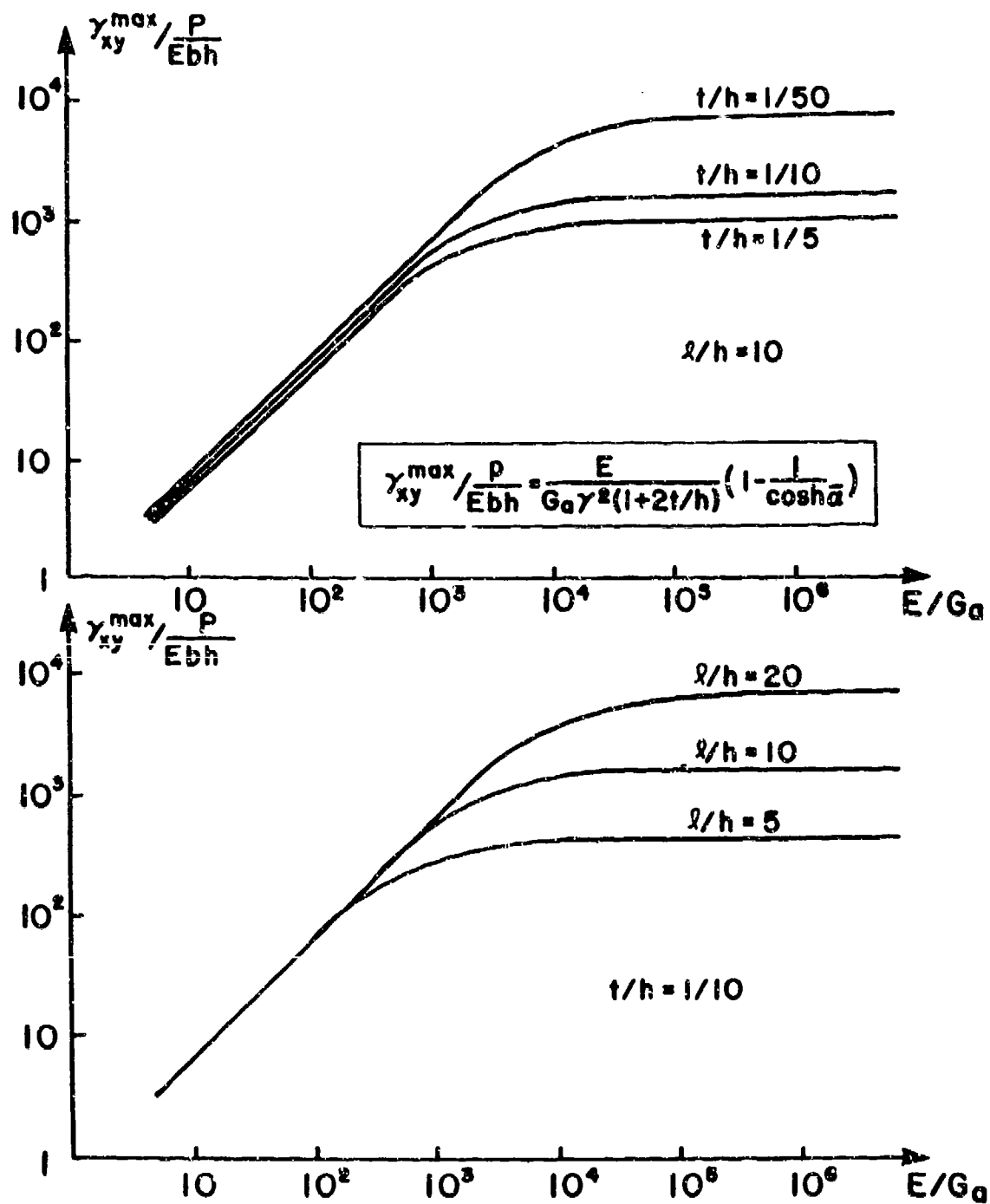


Figure 14. Maximum shear strain in the adhesive layer as a function of adhesive deformability.

Due to the constant maximum shear stress, the shear strain varies linearly in the zone of the "stiffer" adhesives. For the very deformable adhesives an asymptotic value is reached. Here, the adhesive is so deformable that both adherends can develop their full deformation, as if they were individually loaded, without being restricted by the adhesive layer. The value of that  $\gamma_{xy}^{\max}$  corresponds to the relative displacements between the adherends at the loaded end.

From Figures 13 and 14 it is seen that the constant shear stress zone and the linearly varying shear strain zone can be extended by making the beam longer and the adhesive layer thinner. Therefore, for some adhesives, for which a rough estimate of the shear modulus is available, a test geometry can be "tailored" to make sure to be in the linear maximum shear strain zone.

Moreover, making the adhesive layer thinner and the beam longer increases the value of  $\bar{a}$ , thus leading to a constant shear state over a large part of the beam (Figure 12). As a result, shear strain measurements need not be performed at the loaded end of the beam. Moving away from the end will not only make it easier to install the measuring device, but will also eliminate possible end effects.

## 2.4 Deflection of the Bonded Cantilever Beam

### 2.4.1 Integration of the Deflection Equation

In the following section equations will be derived to relate the end deflection of the cantilever or the mid-point deflection of the beam in three-point-bending to the shear modulus of the adhesive. Therefore the deflection equation [2.4],

$$EI \frac{d^2 v}{dx^2} = \frac{P}{2} (\ell - x) - b \frac{h + 2t}{2} \int_x^\ell \tau_{xy}(\eta) d\eta \quad [2.4]$$

must be integrated, using the proper boundary conditions. Substituting the expression for the shear stress in the integral leads to,

$$\begin{aligned}
\frac{d^2v}{dx^2} &= \frac{P}{2EI} (\ell - x) \frac{-b(h+2t)P}{2EIb\gamma^2(h+2t)} \int_x^\ell \left[ 1 - \cosh \frac{\bar{u}\eta}{\ell} + \tanh \bar{u} \sinh \frac{\bar{u}\eta}{\ell} \right] d\eta \\
&= \frac{P}{2EI} (\ell - x) - \frac{P}{2\gamma^2 EI} \left[ \eta - \frac{\ell}{\bar{u}} \sinh \frac{\bar{u}\eta}{\ell} + \frac{\ell}{\bar{u}} \tanh \bar{u} \cosh \frac{\bar{u}\eta}{\ell} \right]_x^\ell \\
&= \frac{P}{2EI} (\ell - x) - \frac{P}{2\gamma^2 EI} \left[ \ell - x + \frac{\ell}{\bar{u}} \sinh \frac{\bar{u}x}{\ell} - \frac{\ell}{\bar{u}} \tanh \bar{u} \cosh \frac{\bar{u}x}{\ell} \right]
\end{aligned} \tag{2.43}$$

Integration of equation [2.43] results in,

$$\begin{aligned}
\frac{dv}{dx} &= \frac{P}{2EI} \left( \ell x - \frac{x^2}{2} - \frac{P}{2\gamma^2 EI} \right. \\
&\left. \left[ \ell x - \frac{x^2}{2} + \left( \frac{\ell}{\bar{u}} \right)^2 \cosh \frac{\bar{u}x}{\ell} - \left( \frac{\ell}{\bar{u}} \right)^2 \tanh \bar{u} \sinh \frac{\bar{u}x}{\ell} \right] \right) + c_1
\end{aligned} \tag{2.44}$$

in which  $C_1$  is an integration constant to be found using boundary conditions. As shown from theory of elasticity (13) or elementary strength of materials (14) approaches, the total deflection of a beam under any kind of loading consists of three terms: a bending term, which is always the dominant term; a shear term, that has some importance only for short beams; and a Poisson term, which is usually two or more orders of magnitude smaller than the dominant one and which depends upon position rather than thickness of the beam. The shear term is due to nonuniform shear stress over the thickness of the adherends, and will be included here.

For a homogeneous monolithic beam, under some unspecified loading resulting in a shear force  $V$ , the shear deflection  $v_s$  is given in differential form by,

$$\frac{dv_s}{dx} = \frac{3V}{2AG} \tag{2.45}$$

where  $A$  is the cross-sectional area of the beam (14, pp. 170-175). In the present case, where the shear force is constant, the shear deflection of the adherends will vary linearly with  $x$ , so that its second derivative will be zero. For the bonded cantilever where each adherend is subjected to a load  $P/2$  and was a cross-sectional area of  $bh$ , equation [2.45] becomes,

$$\frac{dv_s}{dx} = \frac{3P}{4bhG} \tag{2.46}$$

This extra term affects by no means the previously derived deflection equation, since the latter contained only the second derivative of the deflection. However, a note should be made here. Rigorously, this term should also have been included when the boundary condition was used to evaluate the integration constants for the shear stress distribution in the adhesive layer. There, in the first condition,  $dv/dx$  was set to zero at the fixed end, resulting in a vanishing  $\tau_{xy}$  at that end. Later, in section 2.3.5, the physical correctness of that condition was proved. If, on the other hand, the shear term had been included, a singular, and thus physically unacceptable, shear stress in the adhesive layer, at the fixed end, would have been the result; therefore, this secondary deflection term was omitted in the analysis of the shear stress distribution.

The boundary condition for the derivative of the deflection at the fixed end then becomes,

$$\left. \frac{dv}{dx} \right|_{x=0} = \frac{3P}{4bhG} \quad [2.47]$$

Resulting in,

$$c_1 = \frac{P}{2EI\gamma^2} \left( \frac{\ell}{\bar{\alpha}} \right)^2 + \frac{3P}{4bhG} \quad [2.48]$$

and,

$$\begin{aligned} \frac{dv}{dx} = & \frac{P}{2EI} \left( \ell x - \frac{x^2}{2} \right) + \frac{3P}{4bhG} \\ & - \frac{P}{2EI\gamma^2} \left[ \ell x - \frac{x^2}{2} + \left( \frac{\ell}{\bar{\alpha}} \right)^2 \cosh \frac{\bar{\alpha}x}{\ell} - \left( \frac{\ell}{\bar{\alpha}} \right)^2 x - \left( \frac{\ell}{\bar{\alpha}} \right)^2 \tanh \bar{\alpha} \sinh \frac{\bar{\alpha}x}{\ell} \right] \end{aligned} \quad [2.49]$$

Integrate equation [2.49] to find the deflection  $C_2$ , a second integration constant to be found from the boundary condition.

$$\begin{aligned} v = & \frac{P}{2EI} \left[ \frac{\ell x^2}{2} - \frac{x^3}{6} \right] + \frac{3Px}{4bhG} \\ & - \frac{P}{2EI\gamma^2} \left[ \frac{\ell x^2}{2} - \frac{x^3}{6} + \left( \frac{\ell}{\bar{\alpha}} \right)^3 \sinh \frac{\bar{\alpha}x}{\ell} - \left( \frac{\ell}{\bar{\alpha}} \right)^2 x - \left( \frac{\ell}{\bar{\alpha}} \right)^3 \tanh \bar{\alpha} \cosh \frac{\bar{\alpha}x}{\ell} \right] + c_2 \end{aligned} \quad [2.50]$$

Expressing that the deflection is zero at the fixed end, leads to  $C_2$ ,

$$c_2 = - \frac{P}{2EI\gamma^2} \left( \frac{\ell}{\bar{\alpha}} \right)^3 \tanh \bar{\alpha} \quad [2.51]$$

and finally to  $v$ ,

$$v = \frac{P}{2EI} \left[ \frac{\ell x^2}{2} - \frac{x^3}{6} \right] + \frac{3Px}{4bhG} - \frac{P}{2EI\gamma^2} \left[ \frac{\ell x^2}{2} - \frac{x^3}{6} + \left( \frac{\ell}{\bar{\alpha}} \right)^3 \sinh \frac{\bar{\alpha}x}{\ell} - \left( \frac{\ell}{\bar{\alpha}} \right)^2 x - \left( \frac{\ell}{\bar{\alpha}} \right)^3 \tanh \bar{\alpha} \cosh \frac{\bar{\alpha}x}{\ell} + \left( \frac{\ell}{\bar{\alpha}} \right)^3 \tanh \bar{\alpha} \right] \quad [2.52]$$

Equating  $x$  to  $\ell$  and including the current value for the moment of inertia  $I$  of an adherend, the end deflection  $\delta$  of the bonded cantilever beam is obtained. This expression is also the midpoint deflection of a beam in three-point-bending,

$$\begin{aligned} \delta &= \frac{2P\ell^3}{Eb h^3} + \frac{3P\ell}{4bhG} - \frac{6P\ell^3}{Eb h^3 \gamma^2} \left[ \frac{1}{3} + \frac{\sinh \bar{\alpha}}{\bar{\alpha}^3} - \frac{1}{\bar{\alpha}^3} \tanh \bar{\alpha} \cosh \bar{\alpha} + \frac{\tanh \bar{\alpha}}{\bar{\alpha}^3} \right] \\ &= \frac{P\ell^3}{2Eb h} \left[ 4 \left( 1 - \frac{1}{\gamma^2} \right) + \frac{3E}{2G} \left( \frac{h}{\ell} \right)^2 + \frac{12}{\gamma^2} \left( \frac{1}{\bar{\alpha}^2} - \frac{1}{\bar{\alpha}^3} \tanh \bar{\alpha} \right) \right] \end{aligned} \quad [2.53]$$

The factor in front of the parenthesis is exactly the bending term of the deflection of an isotropic cantilever beam of thickness  $2h$ , loaded at the end by a force  $P$ . Expression [2.53] will be slightly modified to have a premultiplier equalling the bending deflection of a cantilever of thickness  $(2h + 2t)$ , so that the term in parenthesis will approach one, if the shear term is not considered, in the case of perfect adhesion,

$$\delta = \frac{P\ell^3}{2Eb(h+t)} (1+t/h)^3 \left[ 4 \left( 1 - \frac{1}{\gamma^2} \right) + \frac{3E}{2G} \left( \frac{h}{\ell} \right)^2 + \frac{12}{\gamma^2} \left( \frac{1}{\bar{\alpha}^2} - \frac{1}{\bar{\alpha}^3} \tanh \bar{\alpha} \right) \right] \quad [2.54]$$

Equation [2.54] can be rewritten as,

$$\delta = \beta \frac{P\ell^3}{2Eb(h+t)^3} \quad [2.55]$$

with,

$$\beta = (1+t/h)^3 \left[ 4 \left( 1 - \frac{1}{\gamma^2} \right) + \frac{3E}{2G} \left( \frac{h}{\ell} \right)^2 + \frac{12}{\gamma^2} \left( \frac{1}{\bar{\alpha}^2} - \frac{1}{\bar{\alpha}^3} \tanh \bar{\alpha} \right) \right] \quad [2.56]$$

The factor  $\beta$  can be seen as a dimensionless end deflection for a bonded cantilever beam, loaded at the end by a force  $P$ . The dependence of this  $\beta$  on the adhesive properties and the significance of each term in the square brackets will be discussed in the next section.

#### 2.4.2 Analysis of the End Deflection Expression

In the previous section, an expression was obtained for the end deflection of a bonded cantilever beam subjected to an endload. Each of the three terms in the square brackets in equation [2.54] or in the definition of  $\beta$  in [2.56] has a distinct physical meaning. The first term is related to the bending of the adherends and is dependent only on geometry. The second is the shear deflection term, and also an adherend- and geometry-related term which is, at most, except for very short beams, a few percent of the bending term. The third and last term is to our purpose the most important because it contains the adhesive properties through parameter  $\bar{\alpha}$ . The magnitude of this term ranges from almost zero for very stiff adhesives to about 4 times the bending term for very deformable adhesives,

$$\beta = (1 + t/h)^3 \left[ 4 \left( 1 - \frac{1}{\gamma^2} \right) + \frac{3E}{2G} \left( \frac{h}{\ell} \right)^2 + \frac{12}{\gamma^2} \left( \frac{1}{\bar{\alpha}^2} - \frac{\tanh \alpha}{\bar{\alpha}^3} \right) \right] \quad [2.56]$$

The variation of coefficient  $\beta$  as a function of the adhesive deformability is shown in Figures 15 and 16 as a function of adhesive thickness and length of the cantilever. A value of 2.6 is taken for  $E/G$ , assuming a Poisson coefficient of 0.3 for the adherends.

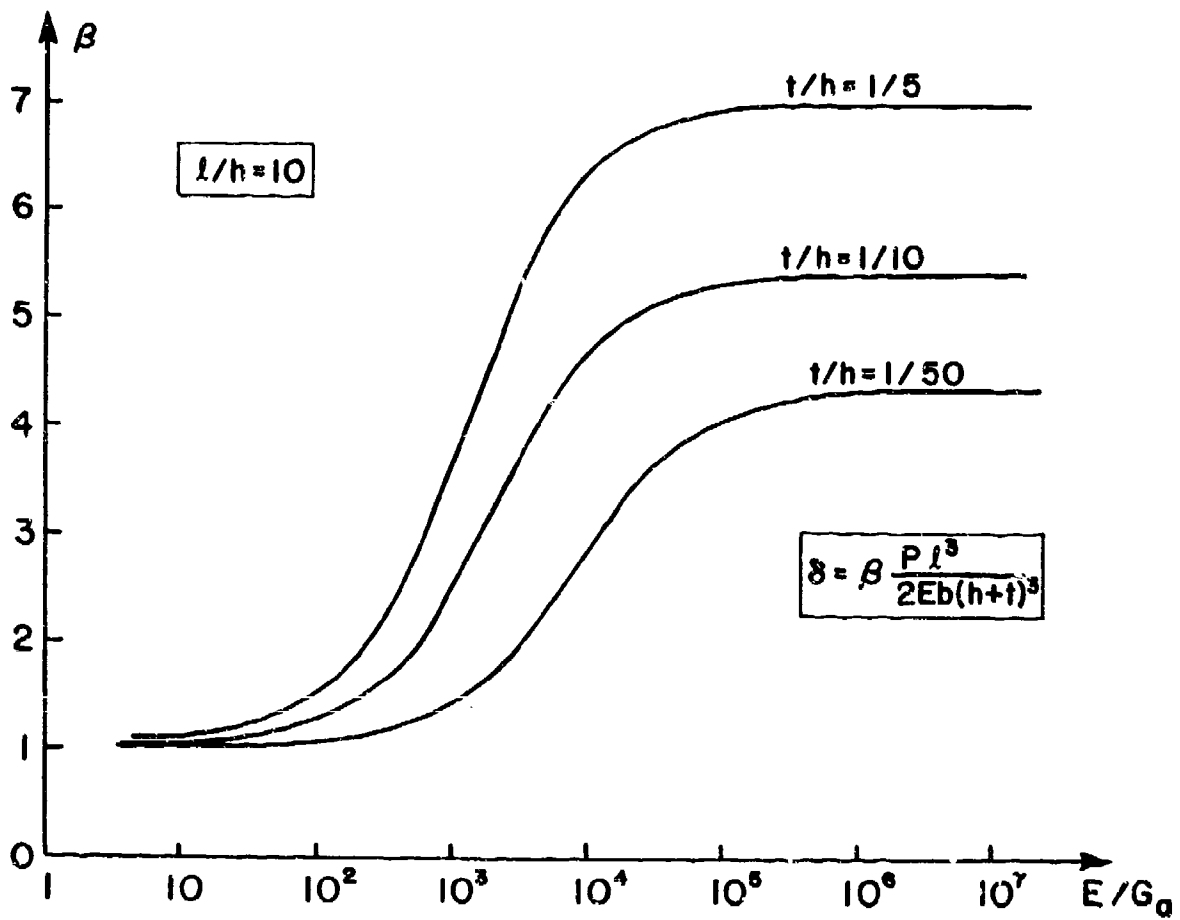


Figure 15. Dependence of the end deflection of the cantilever on the adhesive deformability for various  $t/h$ .

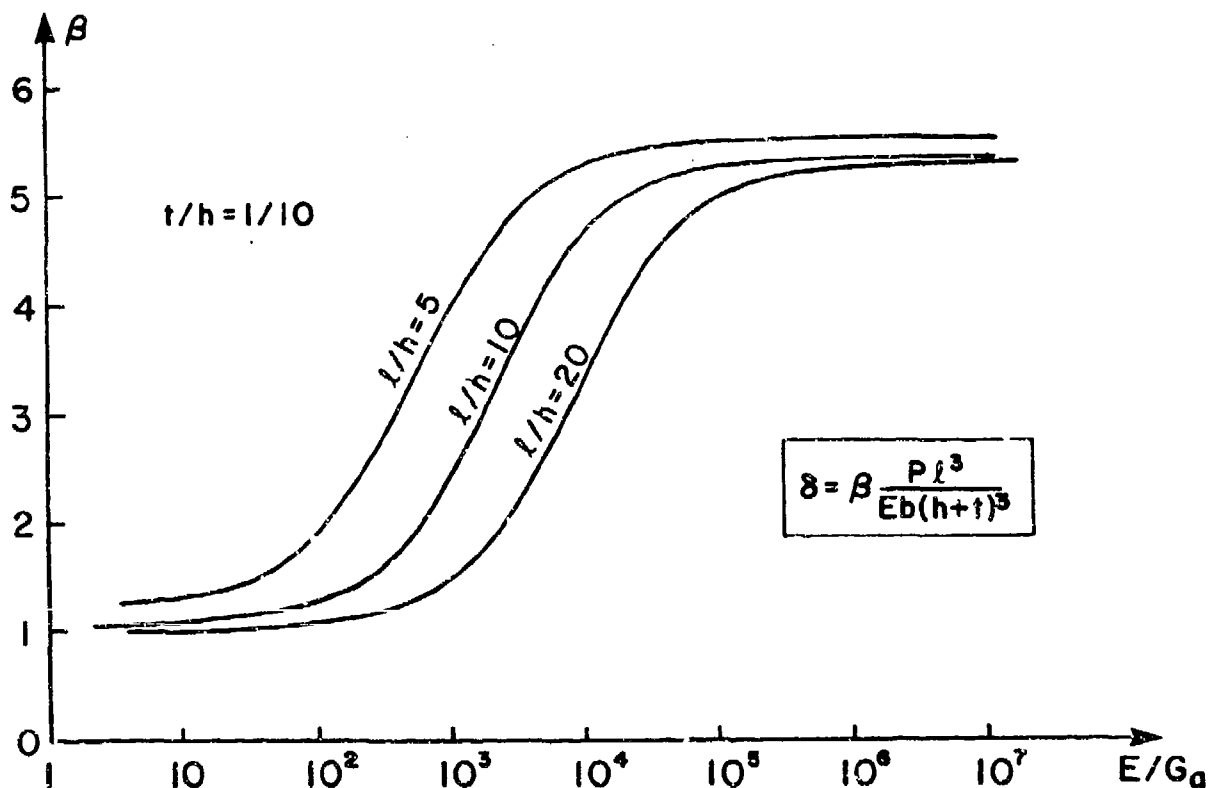


Figure 16. Dependence of the end deflection of the cantilever on the adhesive deformability for various  $l/h$ .

As for the maximum shear stress curves, three zones can be distinguished. For very stiff adhesives, a small zone will exist in which the beam deforms like an isotropic beam which could be referred to as the "perfect adhesion" zone. Here,  $\beta$  is approximately one, if the shear term is not taken into account. On the other side of the graph, for very deformable adhesives, the deflection of two separate beams of thickness  $h$ , each loaded by a force  $P/2$ , is retrieved. For an adhesive thickness of zero, the value of  $\beta$  would be 4 in this zone, because the stiffness of half a beam is an

eighth of the stiffness of the total beam and the load is half the load that is acting on the total beam. That the asymptotic values for  $\beta$  in the graphs are higher than 4 is due to the fact that the isotropic beam is referred to having a thickness  $2(h + t)$  instead of  $2h$ .

These two zones are connected by a high sensitivity zone that is approximately two decades wide. In this middle zone the end deflection is extremely sensitive to the adhesive's shear modulus. Again, the curves can be shifted by changing the geometry of the beam, so that, if a rough estimate of  $G_a$  is available, a specimen can be "tailored" to obtain a deflection in the steep part of the curve. However, as will be discussed below, when it comes to optimizing the specimen for deflection measurements, this shifting doesn't work as well as it did for the shear strain measurements in the adhesive layer itself.

#### 2.4.3 *Experimental Aspects*

The pros and cons of using measurements of the end deflection to obtain the adhesive's shear modulus are discussed in this section.

To give an idea of which adhesive property interval will be of interest for testing purposes, Table 1 gives the  $E/G_a$  ratios for some common adhesives. Generally the adhesives are situated in the "stiff" adhesive zone of Figure 33. Because adhesive layers are usually thin, on the order of 0.005 inch (1.27 mm),  $t/h$  ratios ranging from  $1/20$  to  $1/50$  are common values, meaning that for "fairly long" beams ( $l/h$  ranging from 10 to 20) the beam will be situated in a low sensitivity part of the curve. At most 5 to 10 percent of the total deflection can be related to the adhesive property.

Table 1. Common  $E/G_a$  values for aluminum adherends.

Adhesive	$G_a$ ksi (MPa)	$E/G_a$
Epoxy resins	80-180 (550-1350)	55-125
Polyimides	170 (1200)	60
Phenoxy resins	115-145 (800-1000)	70-90
Rubber polymers*	0.1-1 (1-7)	$3 \cdot 10^4 - 3 \cdot 10^5$

\* bonded to steel

The sensitivity can be increased in two ways, by making the beam shorter or the adhesive layer thicker, both of which can seriously endanger the validity of the underlying theory. For a thick ( $t/h > 1/5$ ) and stiff adhesive layer, the assumption of pure shear in the adhesive should be questioned; for very short beams ( $l/h = 8$  or  $10$ ), the Euler-Bernoulli beam theory is no longer appropriate.

Assuming that an optimized cantilever has an adhesive-adherend thickness ratio of 0.1, and a length to thickness of adherend ratio of 10, the absolute value of the thickness of the adhesive layer becomes important. For a thickness  $2t$  of the adhesive layer of 0.005 inch (0.127 mm), the total thickness of the cantilever would be 0.055 inch (1.40 mm) and its length 0.25 inch (6.35 mm), but these are unrealistic specimen dimensions (Figure 17a). Better dimensions are obtained for an adhesive thickness of 0.04 inch (1.016 mm) (Figure 17b), but still the specimen is small. Therefore, a thick adhesive layer, in absolute value, not in ratio, is crucial to obtain test specimens of reasonable dimensions and good sensitivity.

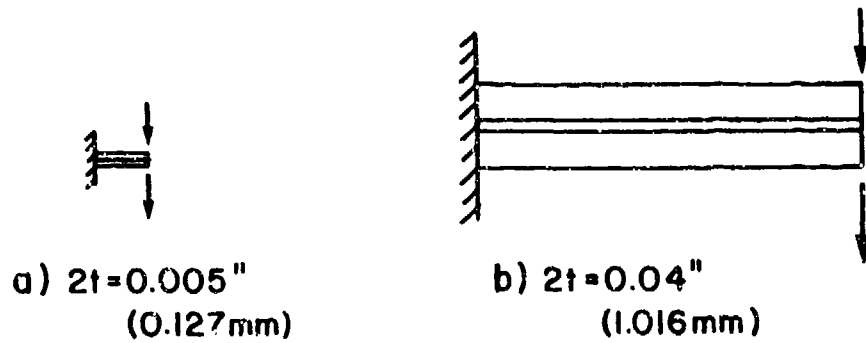


Figure 17. Dependence of the dimensions of a test beam on the absolute value of the thickness of the adhesive layer (scale 1/1).

No single formula is available to obtain the shear modulus  $G_a$  once a measurement of the deflection is made and all geometrical parameters are known. Note that especially the thickness of the adhesive layer must be known with extreme accuracy. There are two possible ways to get to  $G_a$ . The first is to solve equation (2.54) numerically for  $\bar{\alpha}$  and then calculate  $G_a$  using the definition of  $\bar{\alpha}$ ,

$$\delta = \frac{Pl^3}{2EB(h+t)^3} (1+t/h)^3 \left[ 4 \left( 1 - \frac{1}{\gamma^2} \right) + \frac{3E}{2G} \left( \frac{h}{\ell} \right)^2 + \frac{12}{\gamma^2} \left( \frac{1}{\bar{\alpha}^2} - \frac{1}{\bar{\alpha}^3} \tanh \bar{\alpha} \right) \right] \quad [2.54]$$

$$\bar{\alpha} = \frac{\sqrt{3G_a}}{E} \left( \frac{\ell}{h} \right) \frac{(1+2t/h)^2}{t/h} \left( 1 + \frac{1}{3(1+2t/h)^2} \right) \quad [2.57]$$

The second and probably the better way, since it gives a visual idea of accuracy, is a graphical solution for  $G_a$ . From the measured value of  $\delta$ ,  $\beta$  can be calculated. The corresponding part of the  $(E/G_a)$  curve can be magnified for higher accuracy and  $E/G_a$  can be read from the graph (Figure 18).

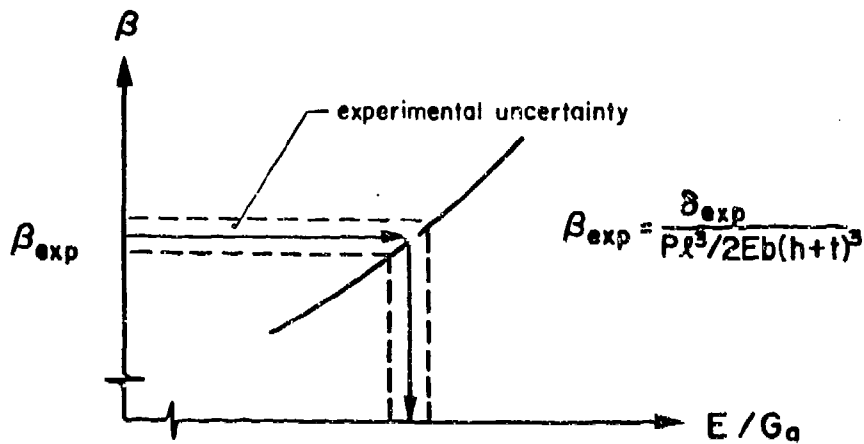


Figure 18. Graphical solution for  $G_a$  from a deflection measurement

The deflection test can also be used to evaluate different types of surface treatments or other factors that influence the state of adhesives. Therefore a coefficient of adhesion is introduced. The deflection of a bonded beam is known to be somewhere between the deflection of a monolithic beam of height  $2(h+t)$  loaded by a force  $P$ , and the deflection of a single adherend of height  $h$  loaded by half that force. These deflections, in their nondimensional form, are shown in Figure 19. The nondimensional end deflection of the bonded cantilever,  $\beta$ , can be seen as the coefficient of adhesion. For  $\beta$  going to unity, the bonded beam will deform in a manner similar to a monolithic beam, thus approaching perfect adhesion. High values of  $\beta$ , on the other hand, mean poor adhesion since the adherends are less restrained in their individual deformation by the presence of the adhesive layer.

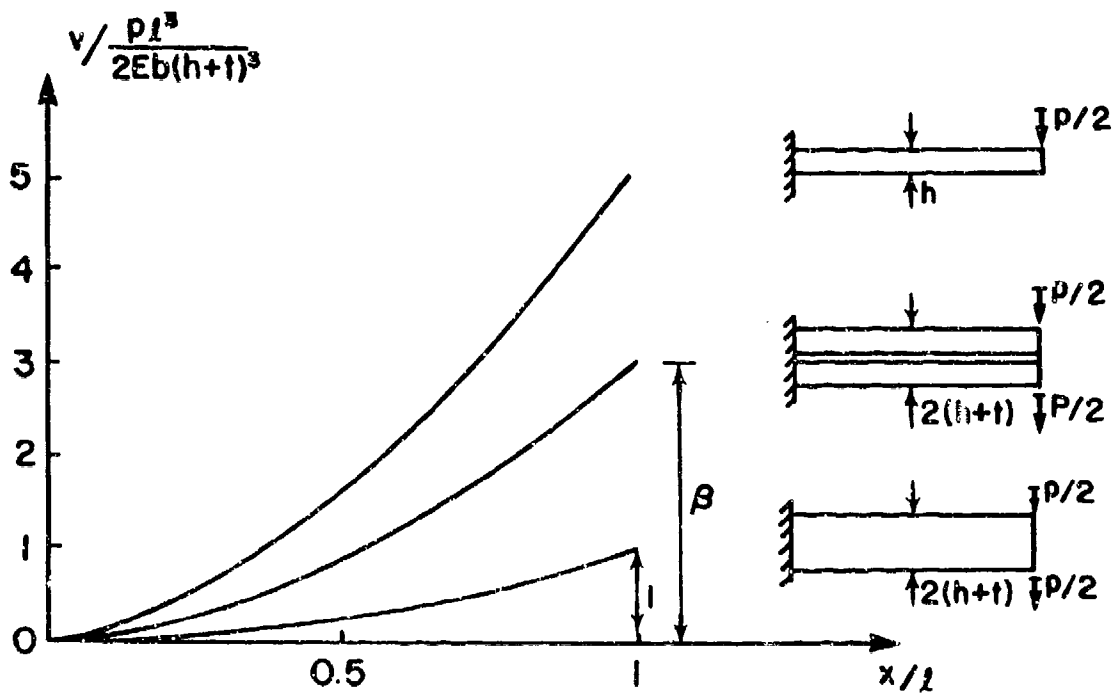


Figure 19. Coefficient of adhesion  $\beta$

Tests to measure  $\beta$  are as easy to perform as the single lap tests that are usually used for quality control. Moreover, this cantilever beam test, provided that it's equally loaded at both adherends, has the advantage over the single lap test in that the adhesive layer really acts in a state of pure shear.

## 2.5 Conclusions

For the adhesively bonded cantilever beam, loaded at the free end, the shear stress in the adhesive layer is not directly related to the externally applied shear force, but to the relative displacements of the adherends on each side of the adhesive layer. The shear stress in the adhesive will always be zero at the fixed end, and for most beams will reach a constant value at some distance away from that end. The magnitude of this shear stress is dependent only on the load and the geometry of the beam for a range of adhesives that were called "stiff" adhesives. This range can be

expanded by making the beam longer and the adhesive layer thinner, thus also approaching a state of constant shear for the whole length of the beam.

For a large part of the beam an almost ideal state of pure and constant shear, the magnitude of which can be calculated from geometry and loading alone, is then obtained. An accurate measurement of the shear strain in the adhesive layer, perhaps with modern optical devices, will easily allow the determination of the adhesive's shear modulus for the assumption of linear elastic adhesive behavior.

The use of deflection measurements to obtain adhesive properties seems less promising, although the test would be easy to perform. Short beams and their adhesive layers are necessary to obtain some sensitivity of the deflection to the adhesive's shear modulus, thus restraining the basic assumptions of the underlying theory and making the shear stress highly dependent on position along the length of the beam. A graphical method was presented to obtain the shear modulus directly from the measurement of the end deflection of the beam.

## 3.0 STRESS-FUNCTION SOLUTION

### 3.1 Introduction

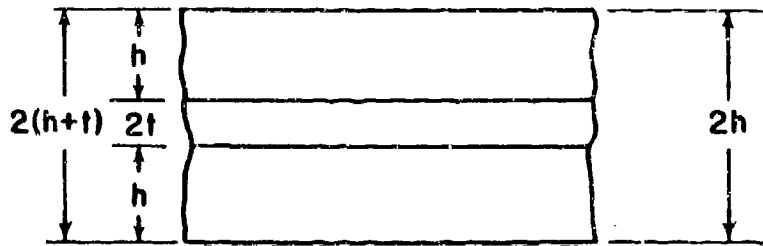
A stress-function approach to a solution for the stress-state in a bonded cantilever beam, loaded at the end, is taken in this chapter. The solution of the previous chapter will be referred to as the strength-of-materials solution. To the three basic assumptions of this strength-of-materials solution -- Euler-Bernoulli beam theory, linear elastic material behavior, and pure shear in the adhesive layer -- a fourth is added. It is assumed that the shear stress in the adhesive layer is constant along the length of the beam.

From the strength-of-materials solution,  $\tau_{xy}$  is known to vary along the length of the beam, going from zero at the fixed end to usually a stable value some distance away. It was also seen that the higher the joint parameter  $\bar{a}$ , the more a state of constant shear for the whole beam is approximated, a high  $\bar{a}$  meaning relatively long beams and thin adhesive layers. For those high  $\bar{a}$  beams, the constant shear assumption may be a reasonable approximation. The consequences of this constant shear assumption are studied in the present chapter.

According to the basic assumption, polynomial stress functions will be proposed for the three layers of the beam. The constants in these stress functions are then to be evaluated using the boundary conditions. Differentiation of the stress-functions twice leads to the stresses in the beam; strains are found using Hooke's law and displacements by integration of the strain expressions. Finally a comparison of both solutions will be made.

A slightly different notation will be used for this stress-function analysis:  $h$  will now be half the thickness of the total beam, including the adhesive layer, whereas  $h$  was the thickness of an adherend only in the strength of materials solution (Figure 20). This change was made not to

confuse the reader, but to obtain the simplest possible expressions in both solution. The cantilever is symmetric with respect to the x-axis, which has its origin at the fixed end. Sub- and superscripts 1, 0 and 2 on stress, strain, and displacement symbols, will refer respectively to the lower adherend, the adhesive layer and the upper adherend respectively (Figure 21).  $G_a$  is the adhesive's shear modulus; the material properties of the adherends carry no subscripts.



**STRENGTH OF  
MATERIALS  
SOLUTION**

**STRESS  
FUNCTION  
SOLUTION**

Figure 20. Definition of  $h$  for both methods.

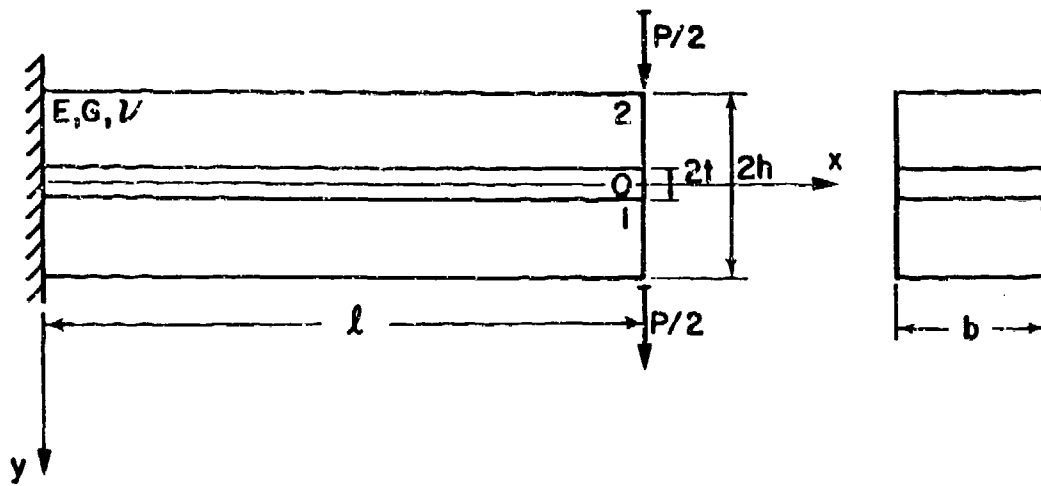


Figure 21. Geometry of the bonded beam for the stress function solution.

### 3.2 Stress State in the Beam

#### 3.2.1 Stress Function Analysis (13)

In an elasticity problem, in this case a two-dimensional plane stress problem, three families of equations need to be solved simultaneously subject to the boundary conditions. These are the equilibrium equations, the compatibility equations, and the constitutive equations.

The stresses existing on a small element of dimension  $dx$  and  $dy$  in a state of plane stress is shown in Figure 22. All stresses are shown in their positive direction. Assuming body forces are zero, the equilibrium equations for this stress state are,

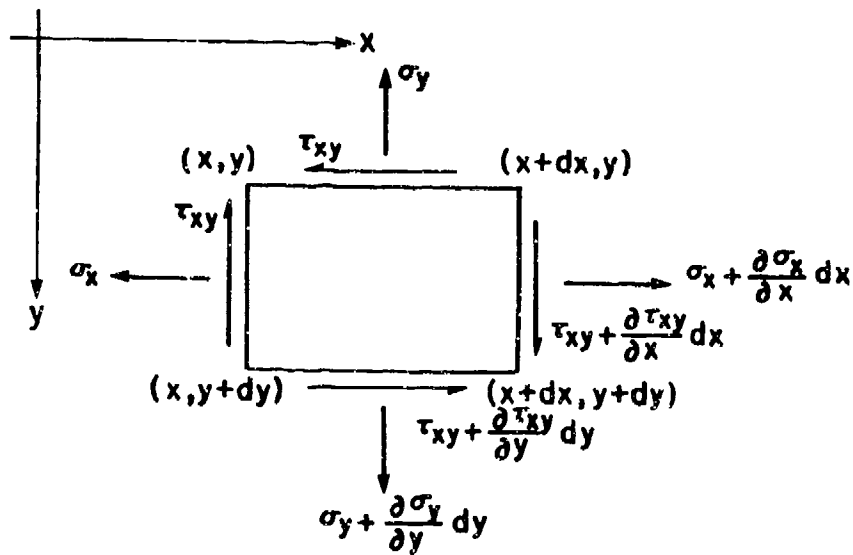


Figure 22. Stresses in a two-dimensional problem.

$$\frac{\partial \sigma_x}{\partial x} + \frac{\partial \tau_{xy}}{\partial y} = 0 \quad [3.1]$$

$$\frac{\partial \sigma_y}{\partial y} + \frac{\partial \tau_{xy}}{\partial x} = 0 \quad [3.2]$$

In order to solve these equations, subject to boundary conditions, the elastic deformation of the body needs to be considered. If  $u$  and  $v$  are the displacement components of some part in the body in the  $x$  and  $y$  directions, respectively, then the three strain components for two dimensional problems are given by,

$$\epsilon_x = \frac{\partial u}{\partial x} \quad [3.3a]$$

$$\epsilon_y = \frac{\partial v}{\partial y} \quad [3.3b]$$

$$\gamma_{xy} = \frac{\partial u}{\partial y} + \frac{\partial v}{\partial x} \quad [3.3c]$$

These three equations can be combined into one which the strain components must obey and which is called the compatibility equation,

$$\frac{\partial^2 \epsilon_x}{\partial y^2} + \frac{\partial^2 \epsilon_y}{\partial x^2} = \frac{\partial^2 \gamma_{xy}}{\partial x \partial y} \quad [3.4]$$

Using Hooke's law,

$$\epsilon_x = \frac{1}{E} (\sigma_x - \nu \sigma_y) \quad [3.5a]$$

$$\epsilon_y = \frac{1}{E} (\sigma_y - \nu \sigma_x) \quad [3.5b]$$

$$\gamma_{xy} = \frac{\tau_{xy}}{G} = \frac{2(1 + \nu)}{E} \tau_{xy} \quad [3.5c]$$

and assuming a plane stress state, the compatibility equation can be expressed in terms of the stress components, resulting in the equation

$$\left[ \frac{\partial^2}{\partial x^2} + \frac{\partial^2}{\partial y^2} \right] [\sigma_x + \sigma_y] = 0 \quad [3.6]$$

To find the stresses, equations [3.1], [3.2] and [3.6] must be solved taking into account the boundary conditions. All this can be done numerically, or analytically by introducing the so-called stress-function,  $\phi$ , defined as:

$$\sigma_x = \frac{\partial^2 \phi}{\partial y^2} \quad [3.7a]$$

$$\sigma_y = \frac{\partial^2 \phi}{\partial x^2} \quad [3.7b]$$

$$\tau_{xy} = - \frac{\partial^2 \phi}{\partial x \partial y} \quad [3.7c]$$

The equilibrium equation [3.1] and [3.2] are then satisfied by definition, so that the stress function only needs to fulfill the compatibility condition, leading to,

$$\frac{\partial^4 \phi}{\partial x^4} + 2 \frac{\partial^4 \phi}{\partial x^2 \partial y^2} + \frac{\partial^4 \phi}{\partial y^4} = 0 \quad [3.8]$$

As stated by Timoshenko and Goodier (13), solutions of [3.8] in the form of polynomials are of interest in the case of "long" rectangular beams, "long" meaning a length-to-stress ratio of 10 or more. How to choose a "suitable" polynomial is the subject of the next section.

### 3.2.2 Choice of the Stress Function Considering the Basic Assumptions

Both adherends and adhesives must be linear elastic; otherwise the stress function method, which explicitly uses Hooke's law, would not be valid. Constant and pure shear is assumed in the adhesive layer. To obtain a state of pure shear, the adhesive layer must be thin and deformable as compared to the adherends. The normal stresses,  $\sigma_x$ , in the adherends are, according to the Euler-Bernoulli beam theory, assumed to vary linearly over the adherend's thicknesses. Also, in the Euler-Bernoulli beam theory there are no transverse normal stresses  $\sigma_y$ .

Three different stress functions,  $\phi_1$ ,  $\phi_2$  and  $\phi_0$ , for each layer of the beam, will be "tailored" to the aforementioned basic assumptions. The coefficients of the terms in the resulting polynomials will have to be found using the boundary conditions on outer surfaces and adherend-adhesive interfaces.

The stress function for the adhesive layer,  $\phi_0$ , is the easiest to obtain. Because of the constant and pure shear assumption, and the definition of the stress function in equation [3.7],  $\phi_0$  will contain only one term and is given as,

$$\phi_0 = e_0 xy \quad [3.9]$$

Lower order terms are useless since they will always be differentiated away. The shear stress in the adhesive layer is then given by,

$$\tau_{xy}^0 = - \frac{\partial^2 \varphi_0}{\partial x \partial y} = - e_0 \quad [3.10]$$

In simple beam theory, the normal stress  $\sigma_x$  is linearly dependent on the applied moment at a certain point along the longitudinal axis. Because the moment in our cantilever beam is a linear function of  $x$ ,  $\sigma_x$  will also be linearly dependent on  $x$ . Moreover,  $\sigma_x$  will be linear in  $y$ . Thus, the proper functional form of  $\sigma_x$  is,

$$\sigma_x = (c_1 x + c_2)(c_3 y + c_4) \quad [3.11]$$

Integrating equation [3.11] twice with respect to  $y$  leads to the general form of the stress function in the adherends,

$$\varphi = c x y^2 + d x y^3 + e x y + f y^2 + g y^3 \quad [3.12]$$

where  $c$ ,  $d$ ,  $e$ ,  $f$ , and  $g$  are constants to be determined.

No quadratic or higher order terms in  $x$  are present because of the condition  $\sigma_y = 0$ . Constant terms or terms linear in  $x$  or  $y$  only are omitted because they do not lead to stresses.

For the lower and upper adherend and for the adhesive layer, respectively, the following stress functions will be used:

$$\varphi_1 = c_1 x y^2 + d_1 x y^3 + e_1 x y + f_1 y^2 + g_1 y^3 \quad [3.13a]$$

$$\varphi_2 = c_2 x y^2 + d_2 x y^3 + e_2 x y + f_2 y^2 + g_2 y^3 \quad [3.13b]$$

$$\varphi_0 = e_0 x y \quad [3.13c]$$

Using the definition of the stress function, the stresses in the beam are given by,

$$\sigma_x^1 = 2c_1 x + 6d_1 x y + 2f_1 + 6g_1 y \quad [3.14a]$$

$$\sigma_x^2 = 2c_2 x + 6d_2 x y + 2f_2 + 6g_2 y \quad [3.14b]$$

$$\tau_{xy}^i = - 2c_1 y - 3d_1 y^2 - e_1 \quad [3.14c]$$

$$\tau_{xy}^2 = -2c_2y - 3d_2y^2 - e_2 \quad [3.14d]$$

$$\tau_{xy}^0 = -e_0 \quad [3.14e]$$

where  $c_i, d_i, e_i, f_i,$  and  $g_i$  are the constants to be evaluated using the boundary conditions.

### 3.2.3 Boundary Conditions

In this section boundary conditions on stresses and displacements will be expressed in terms of the stress function constants leading to a set of linear algebraic equations for which only the results will be given.

The shear stresses along the upper and lower outer surfaces of the adherends are zero:

$$y = h \rightarrow \tau_{xy}^1 = 0 \rightarrow -2c_1h - 3d_1h^2 - e_1 = 0 \quad [3.15]$$

$$y = -h \rightarrow \tau_{xy}^2 = 0 \rightarrow 2c_2h - 3d_2h^2 - e_2 = 0 \quad [3.16]$$

Shear stresses at both side of the adherend-adhesive interface must be equal:

$$y = t \rightarrow \tau_{xy}^0 = \tau_{xy}^1 \rightarrow e_0 = 2c_1t + 3d_1t^2 + e_1 \quad [3.17]$$

$$y = -t \rightarrow \tau_{xy}^0 = \tau_{xy}^2 \rightarrow e_0 = -2c_2t + 3d_2t^2 + e_2 \quad [3.18]$$

Normal stresses on the free ends of the adherends are zero for all values of  $y$ :

$$x = \ell \rightarrow \sigma_x^1 = 0 \rightarrow 2c_1\ell + 6d_1ly + 2f_1 + 6g_1y = 0$$

$$\left[ \begin{array}{l} f_1 = -c_1\ell \\ g_1 = -d_1\ell \end{array} \right. \quad [3.19]$$

$$\sigma_x^2 = 0 \rightarrow 2c_2\ell + 6d_2ly + 2f_2 + 6g_2y = 0 \quad [3.20]$$

$$\left[ \begin{array}{l} f_2 = -c_2 \ell \\ g_2 = -d_2 \ell \end{array} \right. \quad \begin{array}{l} [3.21] \\ [3.22] \end{array}$$

The integral of the shear stresses over the thickness of the beam is equal to the externally applied shear force per unit width of the beam, for each value of  $x$ . In the case of the cantilever loaded at the end, this shear force is constant and equal to  $P$ . Because of the symmetry of the beam about its mid-surface, the integral can be split into two parts, one for the upper and one for the lower half, each equalling half of the applied load.

$$\int_{-h}^h \tau_{xy} dy = \frac{P}{b}$$

$$\left[ \begin{array}{l} \int_{-h}^{-t} \tau_{xy}^2 dy + \int_{-t}^0 \tau_{xy}^0 dy = \frac{P}{2b} \\ \int_0^t \tau_{xy}^0 dy + \int_t^h \tau_{xy}^1 dy = \frac{P}{2b} \end{array} \right.$$

$$\left[ \begin{array}{l} te_0 + c_1(h^2 - t^2) + d_1(h^3 - t^3) + e_1(h - t) = -\frac{P}{2b} \end{array} \right. \quad [3.23]$$

$$\left[ \begin{array}{l} te_0 + c_2(t^2 - h^2) + d_2(h^3 - t^3) + e_2(h - t) = -\frac{P}{2b} \end{array} \right. \quad [3.24]$$

Equations [3.15] to [3.24] now provide ten equations in the eleven unknown constants. Those ten conditions are all stress-related, none of them containing material properties. The last condition will have to express compatibility of displacements on each side of the adhesive layer. The relative displacements of opposite points on the adhesive-adherend interfaces must be related to the shear strain in the adhesive layer (Figure 23). Obtaining this condition will require elaborate calculations, and it will even be proved to be impossible to satisfy such a continuity condition for the whole length of the beam due to the constant shear stress assumption. By definition, the engineering shear strain in the adhesive layer  $\gamma_{xy}^0$ , is given by,

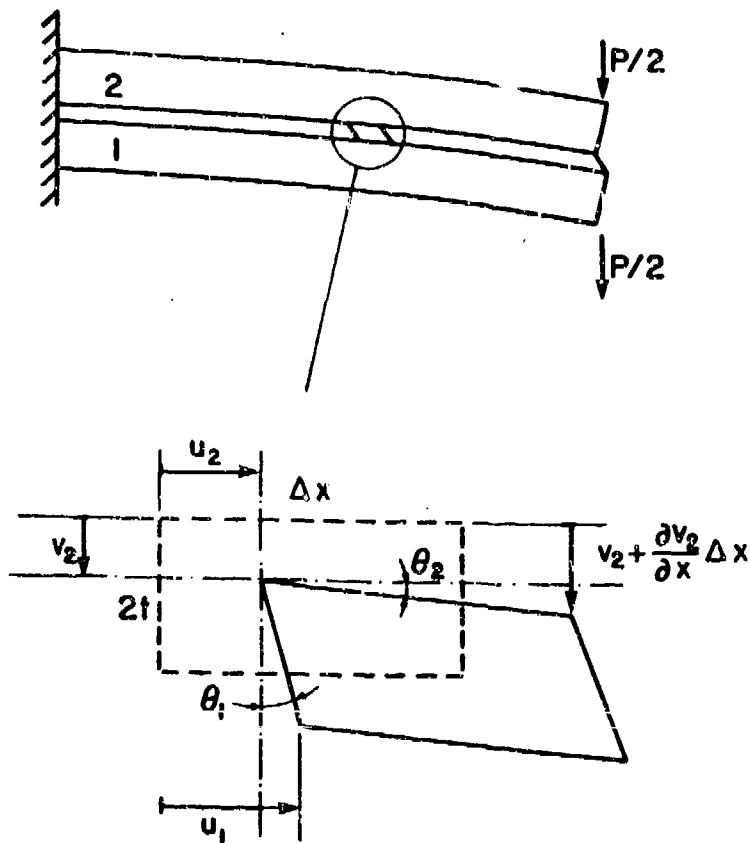


Figure 23. Deformation of an element of adhesive in the adhesive layer.

$$\gamma_{xy}^0 = \theta_1 + \theta_2 \quad [3.25]$$

or, assuming small angles,

$$\gamma_{xy}^0 = \frac{\Delta u}{2t} + \frac{v_2 + \frac{\partial v_2}{\partial x} \Delta x - v_2}{\Delta x} \quad [3.26]$$

where  $\Delta u$  is the horizontal component of the relative displacement of two opposing points on either side of the adhesive layer, and  $v_2$  is the vertical displacement of the interface point on the upper adherend.

$$\Delta u = u_1(y = t) - u_2(y = -t) \quad [3.27]$$

The compatibility condition is then,

$$\gamma_{xy}^0 = \frac{\Delta u}{2t} + \frac{\partial v_2}{\partial x} \quad [3.28]$$

Using the expressions for the stresses in the adherends and equations [3.14], together with Hooke's law and considering that there are no vertical normal stresses, the displacement fields in the adherends can be obtained by integration of the normal strains. Equations [3.21] and [3.22] are also used.

$$\begin{aligned} v_2 &= \int \epsilon_y^2 dy = -\frac{\nu}{E} \int [2c_2(x - \ell) + 6d_2y(x - \ell)] dy \\ &= -\frac{\nu}{E} (2c_2y + 3d_2y^2)(x - \ell) + V_2(x) \end{aligned} \quad [3.29]$$

Similarly,

$$v_1 = -\frac{\nu}{E} (2c_1y + 3d_1y^2)(x - \ell) + V_1(x) \quad [3.30]$$

The horizontal displacements are obtained by integration of  $\epsilon_x$ ,

$$u_1 = \int \epsilon_x^1 dx = \frac{1}{E} (c_1x^2 + 3d_1x^2y - 2c_1\ell x - 6d_1\ell xy) + U_1(y) \quad [3.31]$$

$$u_2 = \int \epsilon_x^2 dx = \frac{1}{E} (c_2x^2 + 3d_2x^2y - 2c_2\ell x - 6d_2\ell xy) + U_2(y) \quad [3.32]$$

$U_1(y)$ ,  $U_2(y)$ ,  $V_1(x)$  and  $V_2(x)$  are to be evaluated using compatibility equations [3.33] within each adherend, together with the boundary condition on the displacements ( $i = 1$  or  $2$ ).

$$\frac{\partial u_i}{\partial y} + \frac{\partial v_i}{\partial x} = \gamma_{xy}^i = \frac{\tau_{xy}^i}{G} \quad [3.33]$$

Substitution of the displacement expressions in this equation results, for the lower adherend, in,

$$F(x) + G(y) = -\frac{e_1}{G} \quad [3.34]$$

where

$$F(x) = \frac{dV_1(x)}{dx} + \frac{1}{E}(3d_1x^2 - 6d_1lx) = k_1 \quad [3.35]$$

$$G(y) = \frac{dU_1(y)}{dy} + \frac{2c_1y}{G} + \frac{3d_1y^2}{G} - \frac{\nu}{E}(2c_1y + 3d_1y^3) = k_2 \quad [3.36]$$

The right-hand side of equation [3.34] is a constant and, because the sum of the independent functions  $F(x)$  and  $G(x)$  is a constant, each function must be a constant also. Equations [3.35] and [3.36] are then integrated to find  $U_1(y)$  and  $V_1(x)$ , in which expressions four integration constants,  $K_1$  to  $K_4$ , remain to be evaluated. Replacing  $U_1(y)$  and  $V_1(x)$  in equation [3.30] and [3.31] results in the following displacements,

$$u_1 = \frac{1}{E}(c_1x^2 + 3d_1x^2y - 2c_1lx - 6d_1lxy) + k_2y + k_4 + \frac{\nu}{E}(c_1y^2 + d_1y^3) - \frac{c_1}{G}y^2 - d_1\frac{y^3}{G} \quad [3.37]$$

$$v_1 = -\frac{\nu}{E}(2c_1y + 3d_1y^2)(x - l) + k_1x + k_3 - \frac{1}{E}(d_1x^3 - 3d_1lx) \quad [3.38]$$

Usually, for isotropic beams, boundary conditions for displacements are evaluated at the midsurface of the beam or, for simple bending, the neutral axis, which position is an unknown in the case of the bonded cantilever. What is known is that the neutral surface must lie somewhere between the midsurface of each adherend and the midsurface of the bonded beam. In order to retrieve the deflection of an isotropic beam in the perfect adhesion case, the boundary conditions are expressed for  $x$  and  $y$  equal to zero. This is an artificial choice since the origin is no part of the adherends if an adhesive layer is present, but leading to acceptable results.

The boundary conditions are that there is no vertical or horizontal displacement at the origin and that a vertical element should stay vertical after deformation. The latter condition implies that the derivative of the horizontal displacement with respect to  $y$  must be zero ((13), pp. 41-46).

$$\text{at } \begin{matrix} x = 0 \\ y = 0 \end{matrix} \rightarrow \begin{cases} u = 0 \\ v = 0 \\ \frac{\partial u_1}{\partial y} = 0 \end{cases} \quad [3.39]$$

The resulting integration constants are,

$$k_2 = k_3 = k_4 = 0 \text{ and } k_1 = -\frac{e_1}{G} \quad [3.40]$$

which when substituted in equations [3.37] and [3.38] give the following displacements in the lower adherend,

$$u_1 = \frac{1}{E}(c_1x^2 + 3d_1x^2y - 2c_1\ell x - 6d_1\ell xy) + \frac{v}{E}(c_1y^2 + d_1y^3) - \frac{c_1}{G}y^2 - \frac{d_1y^3}{G} \quad [3.41]$$

$$v_1 = -\frac{v}{E}(2c_1y + 3d_1y^2)(x - \ell) - \frac{e_1}{G}x - \frac{1}{E}(d_1x^2 - 3d_1\ell x) \quad [3.42]$$

Similarly for the upper adherend,

$$u_2 = \frac{1}{E}(c_2x^2 + 3d_2x^2y - 2c_2\ell x - 6d_2\ell xy) + \frac{v}{E}(c_2y^2 + d_2y^3) - \frac{c_2}{G}y^2 - \frac{d_2y^3}{G} \quad [3.43]$$

$$v_2 = -\frac{v}{E}(2c_2y + 3d_2y^2)(x - \ell) - \frac{e_2}{G}x - \frac{1}{E}(d_2x^2 - 3d_2\ell x) \quad [3.44]$$

Using these displacements, the right-hand side of the compatibility condition [3.28] will be an expression containing terms in  $x$  and  $x_2$  as well as constants.

$$\frac{u_1(y = t) - u_2(y = -t)}{2t} + \frac{\partial v_2}{\partial x}(y = -t) = f(x^0, x^1, x^2) \quad [3.45]$$

If compatibility is satisfied everywhere along the length, this function  $f$  should equal  $\gamma_y^0$  for each value of  $x$ , an impossible result because of the assumption of constant shear stress (and hence constant shear strain) in the adhesive layer. Thus, the price paid for the constant shear stress assumption is that compatibility of displacements through the adhesive thickness will not be satisfied

everywhere. In fact the condition can only be satisfied in one point, or at most two, since equation [3.46] is a quadratic one.

$$f(x^0, -1, x^2) = \gamma_{xy}^0 = \frac{\tau_{xy}^0}{G_a} \quad [3.46]$$

From the strength-of-materials solution the shear stress is known to be constant, in most cases, for a part of the beam near the loaded end. Therefore the one point, for which the condition will be assumed to be satisfied, will be the end point,  $x = \ell$ , Equation [3.46] expressed at  $x = \ell$ , will then provide the eleventh and last equation in the eleven unknown stress-function constants.

$$\begin{aligned} & \frac{1}{E}(-c_1\ell^2 - 3d_1\ell^2\ell) + \frac{\nu}{E}(c_1\ell^2 + d_1\ell^3) - \frac{c_1\ell^2}{G} - \frac{d_1\ell^3}{G} \\ & - \left[ \frac{1}{E}(-c_2\ell^2 + 3d_2\ell^2\ell) + \frac{\nu}{E}(c_2\ell^2 - d_2\ell^3) - \frac{c_2\ell^2}{G} + \frac{d_2\ell^3}{G} \right] \\ & + 2\ell \left[ -\frac{\nu}{E}(-2c_2\ell + 3d_2\ell^2) - \frac{e_2}{G} + \frac{3d_2\ell^2}{E} \right] = -\frac{2\ell e_0}{G_a} \end{aligned} \quad [3.47]$$

Solution of the set of linear algebraic equations results in,

$$d_1 = d_2 = \frac{P}{2bh^3} \frac{N}{D} \quad [3.48]$$

$$f_1 = -f_2 = -c_1\ell = c_2\ell = -\frac{P\ell}{2bh^2} \frac{1}{1-\omega^3} \left[ 1 - \frac{2N}{D}(1-\omega^2) \right] \quad [3.49]$$

$$g_1 = g_2 = -\frac{P\ell}{Ebh^3} \frac{N}{D} \quad [3.50]$$

$$e_1 = e_2 = -\frac{P}{bh} \frac{1}{1-\omega^2} \left[ L - \frac{2N}{D}(1-\omega^3) \right] - \frac{3}{2} \frac{P}{bh} \frac{N}{D} \quad [3.51]$$

$$e_0 = -\frac{P}{bh} \frac{1}{1+\omega} \left[ 1 - \frac{2N}{D}(1-\omega^3) \right] - \frac{3}{2} \frac{P}{bh} (1-\omega^2) \frac{N}{D} \quad [3.52]$$

in which,

$$\omega = \frac{\ell}{h} \quad [3.53]$$

$$N = 1 + 2\frac{E}{G_a}\left[\frac{h}{\ell}\right]^2\omega(1-\omega) - \frac{E}{G}\left[\frac{h}{\ell}\right]^2\omega(2-\omega) + \nu\omega^2\left[\frac{h}{\ell}\right]^2 \quad [3.54]$$

$$D = 2(1-\omega^3) + \frac{E}{G_a}\left[\frac{h}{\ell}\right]^2\omega(1-\omega)^4 - \frac{E}{G}\left[\frac{h}{\ell}\right]^2\omega(1-\omega)(1-\omega+3\omega^2-\omega^3) + 2\nu\left[\frac{h}{\ell}\right]^2\omega^2(1-\omega) \quad [3.55]$$

To each term in both N and D, a physical meaning can be attached. The first term is related to bending deformation of the adherends, the second to the presence of the adhesive layer, the third to the shear deformation of the adherends, and the last to Poisson effects. In the case of relatively stiff adhesives, such as epoxies, there is roughly an order-of-magnitude-difference between any two consecutive terms, decreasing from the bending to the Poisson term. This difference is for beams that are not too long.

Now that the constants have been found, all stresses and displacements in adherends and adhesive can be obtained by simple substitution in the appropriate aforementioned expressions.

Note again that this solution is an approximate solution, satisfying all equilibrium conditions, satisfying compatibility within each layer separately, but satisfying compatibility of displacements on both sides of the adhesive layer in only one point. Increasing the order of the polynomial for the stress function,  $\varphi_0$ , could account for a varying shear stress in the adhesive layer that would immediately imply that the dependence of the normal stresses on  $x$  in the adherends would no longer be linear, thus requiring higher order polynomials for the adherend's stress functions. The only result would be for the analysis to become more laborious and expressing the through-the-adhesive-compatibility would lead to a higher order equation than quadratic in  $x$ . These results would mean that compatibility could never be completely satisfied using polynomial stress functions.

### 3.2.4 Shear Stress in the Adhesive Layer

Because the shear stress in the adhesive equals minus  $\epsilon_0$ ,  $\tau_{xy}^0$  is found immediately to be,

$$\tau_{xy}^0 = \frac{P}{bh} \frac{1}{1 + \omega} \left[ 1 - \frac{2N}{D} (1 - \omega^3) \right] + \frac{3P}{2bh} (1 - \omega^2) \frac{N}{D} \quad [3.56]$$

In section 4 of this chapter, the shear stress given by equation [3.56] will be compared to the maximum shear stress in the adhesive layer as obtained in the strength-of-materials solution. It will also be determined whether expression [3.56] can be related to the simple cases of perfect adhesion and no adhesion.

Hypothetically, the case of perfect adhesion is encountered when the thickness of the adhesive layer, or its dimensionless form,  $\omega$ , approaches zero, as shown below.

$$\lim_{\omega \rightarrow 0} \frac{N}{D} = \frac{1 + 0 + 0 + 0}{2 + 0 + 0 + 0} = \frac{1}{2} \quad [3.57]$$

$$\lim_{\omega \rightarrow 0} \tau_{xy}^0 = \frac{P}{bh} (1 - 1) + \frac{3P}{4bh} = \frac{3P}{4bh} \quad [3.58]$$

Obviously, after taking the necessary limits, the maximum shear stress at the midsurface of an isotropic cantilever is retrieved. For the case of no adhesion,  $G_a$  approaches zero, making the second term in N and D the dominant one. Taking the double limit for both  $G_a$  and  $\omega$  going to zero,  $\tau_{xy}^0$  is logically found to be vanishing.

$$\lim_{\substack{G_a \rightarrow 0 \\ \omega \rightarrow 0}} \frac{N}{D} = \lim_{\substack{G_a \rightarrow 0 \\ \omega \rightarrow 0}} \frac{\frac{2E}{G_a} \left[ \frac{h}{\ell} \right]^2 \omega(1 - \omega)}{\frac{E}{G_a} \left[ \frac{h}{\ell} \right]^2 \omega(1 - \omega)^4} = 2 \quad [3.59]$$

$$\lim_{\substack{G_a \rightarrow 0 \\ \omega \rightarrow 0}} \tau_{xy}^0 = \frac{P}{bh} [1 - 4] + \frac{3P}{2bh} \times 2 = 0 \quad [3.60]$$

### 3.3 Deflection of the Cantilever

Replacing the stress function constants by their solution in equations [3.42] or [3.44] results in the wanted deflection equation. If transverse effects are ignored, each point of the beam for a certain  $x$  moves downward the same amount.

$$v = -\frac{e_1}{G}x - \frac{d_1}{E}(x^3 - 3\ell x^2) \quad [3.61]$$

$$v = \frac{Px}{Gbh} \frac{1}{1-\omega^2} \left[ 1 - \frac{2N}{D}(1-\omega^3) \right] + \frac{3}{2} \frac{Px}{Gbh} \frac{N}{D} - \frac{P}{2Eb^3} \frac{N}{D}(x^3 - 3\ell x^2) \quad [3.62]$$

The end deflection,  $\delta$ , is then,

$$\delta = \frac{P\ell^3}{Eb^3} \frac{N}{D} + \frac{P\ell}{Gbh} \left[ \frac{1}{1-\omega^2} - \frac{2N}{D} \frac{1-\omega^3}{1-\omega^2} + \frac{3N}{2D} \right] \quad [3.63]$$

Like for the strength-of-materials solution, graphs can be made of  $\delta$  as a function of the adhesive deformability for various adhesive thicknesses and beam lengths. Because the strength of materials approach is obviously the more acceptable solution, only one case will be examined for comparison in the next section.

$\delta$  can also be written as a bending deflection factor multiplied by a dimensionless coefficient,  $\bar{\beta}$ , as in the earlier solution.

$$\delta = \beta \frac{P\ell^3}{2Eb^3} \quad [3.64]$$

$$\bar{\beta} = \frac{2N}{D} + \frac{2E}{G} \left[ \frac{h}{\ell} \right]^2 \left[ \frac{1}{1-\omega^2} - \frac{2N}{D} \frac{1-\omega^3}{1-\omega^2} + \frac{3N}{2D} \right] \quad [3.65]$$

### 3.4 Comparison of the Two Solutions

A graphical comparison of the dependence on the adhesive's deformability of the shear stress in the adhesive and the end deflection of the beam will be made for a beam of a given geometry. Expressed in the notations of this chapter, its characteristics will be:  $t/h = 0.1$  and  $l/h = 10$ .

In order to compare equivalent quantities, the dimensionless shear stresses  $\tau$  and the dimensionless end deflections  $\beta$  have to be expressed for an identical definition of  $h$ . In Chapter 2, the maximum shear stress in the adhesive layer,  $\tau_{xy}^{\max}$ , and the end deflection,  $\delta$ , were found to be,

$$\tau_{xy}^{\max} = \frac{P}{bh\gamma^2} \frac{1}{(1 + 2l/h)} \left[ 1 - \frac{1}{\cosh \bar{\alpha}} \right] \quad [2.41]$$

$$\delta = \beta \frac{Pl^3}{2Ebh^3(1 + l/h)^3} \quad [2.56]$$

In these expressions, all parameters containing  $h$  need to be transformed to the definition of  $h$  in this chapter, which are half the thickness of the total beam. This process is cumbersome and not too relevant and leads to,

$$\tau_{xy}^{\max} = \tau^* \frac{P}{bh} \quad [3.66]$$

and

$$\delta = \beta^* \frac{P}{2Ebh^3} \quad [3.67]$$

In equations [3.65] and [3.67],  $\tau^*$  and  $\beta^*$  are the transformed dimensionless maximum shear stress in the adhesive and the transformed dimensionless end deflection of the beam. They are compared, in Figures 24 and 25, to their equivalents,  $\bar{\tau}$  and  $\bar{\beta}$ , as obtained in the stress function solution.

$$\tau_{xy}^0 = \frac{P}{bh} \frac{1}{1 + \omega} \left[ 1 - \frac{2N}{D} (1 - \omega^3) \right] + \frac{3P}{2bh} (1 - \omega^2) \frac{N}{D} \quad [3.56]$$

$$\rightarrow \tau_{xy} = \bar{\tau} \frac{P}{bh} \quad [3.68]$$

and

$$\delta = \bar{\beta} \frac{Pl}{2Ebh^3} \quad [3.69]$$

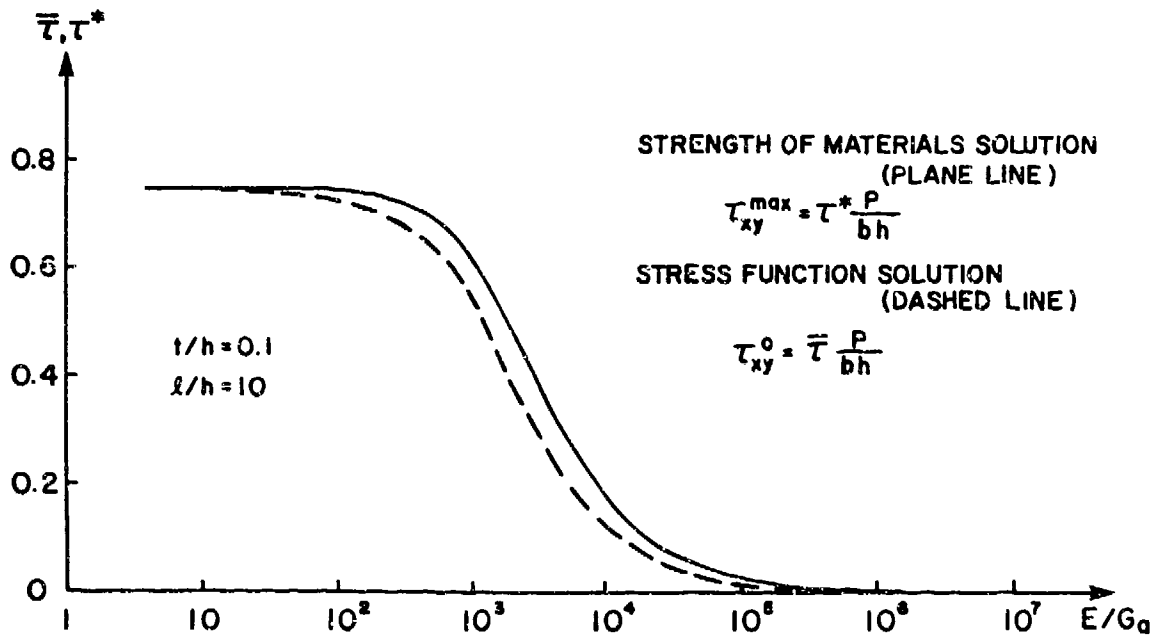


Figure 24. Comparison of the shear stress in the adhesive for the two solutions.

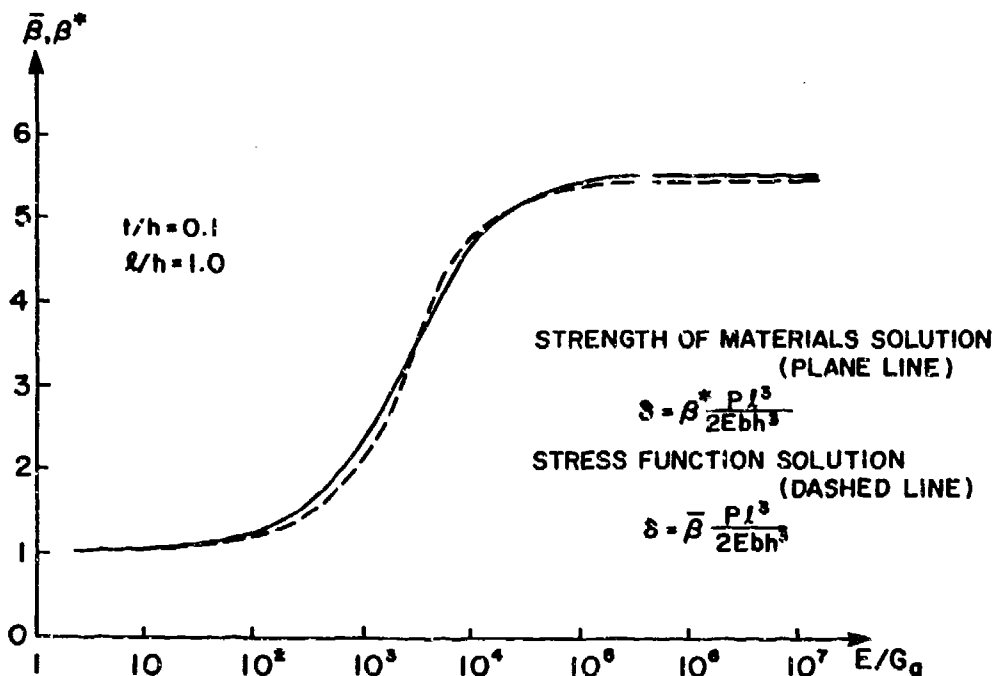


Figure 25. Comparison of the end deflection of the beam for both solutions.

Generally, both solutions show good agreement, especially for the end deflection values in Figure 25. In each figure, identical asymptotic values are reached and major changes occur for the same interval of adhesive deformability  $E/G_a$ . To obtain an estimate of the end deflection or the maximum shear strain in the adhesive layer of a bonded cantilever, both solutions can be used. When it comes to using these quantities to actually calculate the adhesive shear modulus, slight changes in shear stress or deflection can lead to huge differences in adhesive properties. Therefore, the solution based on the less restraining assumption - the strength-of-materials solution, in other words - should be preferred over the other.

Other geometries such as those used for this comparison lead to similar graphs. They will be only somewhat shifted along the horizontal axis, like the curves presented in Chapter 2.

### 3.5 Conclusions

In this chapter, a stress function solution, based on a hypothetical constant shear state in the adhesive layer, was presented. That restraining assumption led to incomplete satisfaction of the compatibility condition on displacements on both sides of the adhesive layer. Therefore this solution should be handled with some caution.

When compared to the strength-of-materials solution, both solutions showed good general agreement. The differences that were noted, however, proved too important to enable use of the stress function solution to calculate the adhesives' shear modulus. The strength-of-materials solution is to be preferred over the stress-function solution because of its less restraining assumptions.

## 4.0 NUMERICAL EVALUATION OF THE STRENGTH OF MATERIALS SOLUTION

### 4.1 Introduction

The strength of materials solution as presented in Chapter 2 will be evaluated using the finite element code VISTA. The elements used are 8-node isoparametric quadrilateral elements. Horizontally the cantilever is subdivided into 16 elements with refinements towards both the loaded and the fixed ends; vertically the adherends and adhesive layer each contain 4 elements (Figure 26).

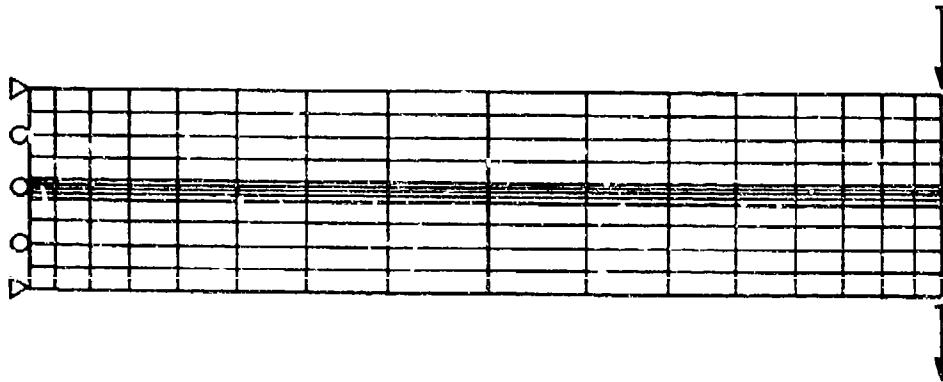


Figure 26. Discretization of the beam.

---

For a number of geometries the shear stress distribution in the adhesive layer and the end deflection are analyzed, and the results are summarized in Table 2. Starting from a "standard beam" (case 3 in the table) for each run one of the beam characteristics, either the slenderness of the beam, the thickness of the adhesive layer, or the stiffness of the adhesive, was changed.

#### 4.2 Shear Stress in the Adhesive Layer (Table 2)

Three features of the shear stress distribution in the adhesive layer will be discussed: its variation along the length and over the thickness of the adhesive layer, and its dependence on geometrical and adhesive parameters.

For cases 1, 3 and 4 in Table 2, the shear stress in the middle of the adhesive layer as obtained using finite elements is compared to the analytical solution in Figure 27. In this figure, two features catch the eye: first and most important, the excellent agreement between numerical and theoretical values; and, second that something happens to the numerical shear stress at the loaded end of the beam. The reason for this numerical instability is the very high stress gradient at the extreme end of the adhesive layer. Since the outer surface of the adhesive layer is free of stresses, the shear stress in the adhesive layer should drop "instantly," meaning over a very short distance, from its maximum value to zero, for  $x$  is equal to  $l$ . This end effect cannot be included in the strength-of-materials solution and can only be accurately evaluated with a highly refined element mesh in the neighborhood of the singularity.

Table 2. Overview of numerical study (the adherends are aluminum,  $E = 10^7$  psi)

Case no.	$l$ (inch)	$h$ (inch)	$z/h$	$t$ (inch)	$t/h$	$E/G_a$	$\bar{\alpha}$	$\tau_{xy}^{\max}$ Fin. El. (psi)	$\tau_{xy}^{\max}$ Theor. (psi)	$\delta$ Fin. El. (inch)	$\delta$ Theor. (inch)
1	2.5	0.25	10	0.025	0.1	26	14.33	271	271	$3.77 \cdot 10^{-3}$	$4.16 \cdot 10^{-3}$
2	2.5	0.25	10	0.025	0.1	87	7.83	271	271	$4.24 \cdot 10^{-3}$	$4.63 \cdot 10^{-3}$
3	2.5	0.25	10	0.025	0.1	260	4.52	266	265	$5.38 \cdot 10^{-3}$	$5.79 \cdot 10^{-3}$
4	2.5	0.25	10	0.025	0.1	2600	1.43	144	148	$12.08 \cdot 10^{-3}$	$12.92 \cdot 10^{-3}$
5	2.5	0.25	10	0.025	0.1	26000	0.45	23	25	$17.33 \cdot 10^{-3}$	$18.98 \cdot 10^{-3}$
6	2.5	0.25	10	0.0125	0.05	260	5.97	283	284	$5.16 \cdot 10^{-3}$	$5.43 \cdot 10^{-3}$
7	2.5	0.25	10	0.005	0.02	260	9.03	295	294	$4.93 \cdot 10^{-3}$	$5.66 \cdot 10^{-3}$
8	5.0	0.25	20	0.025	0.1	260	9.04	271	271	$31.79 \cdot 10^{-3}$	$34.56 \cdot 10^{-3}$

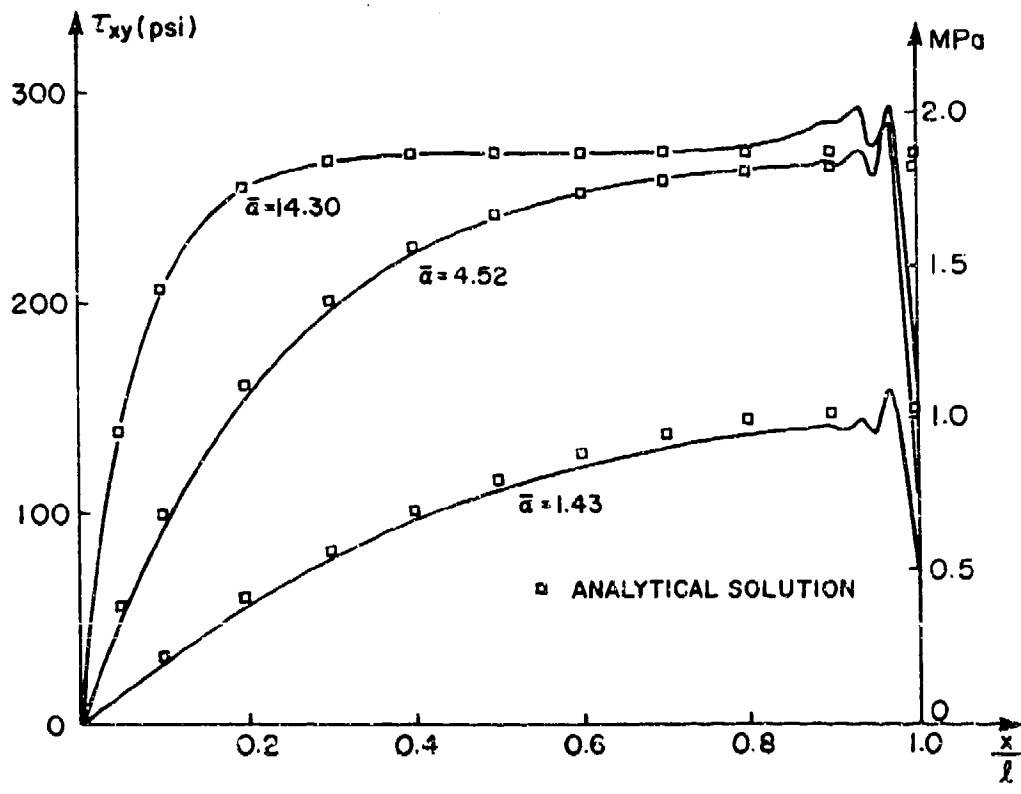


Figure 27. Comparison of numerically and theoretically obtained shear stress.

One of the basic assumptions of the strength-of-materials solution was that the adhesive acts in a state of pure shear; in other words that the shear stress does not vary over the adhesive thickness. This assumption is numerically confirmed in Figure 28. In this figure, the "variation" of the shear stress over the adhesive thickness for various positions along the length of the beam is pictured, showing only a very slight change in magnitude near the loaded end.

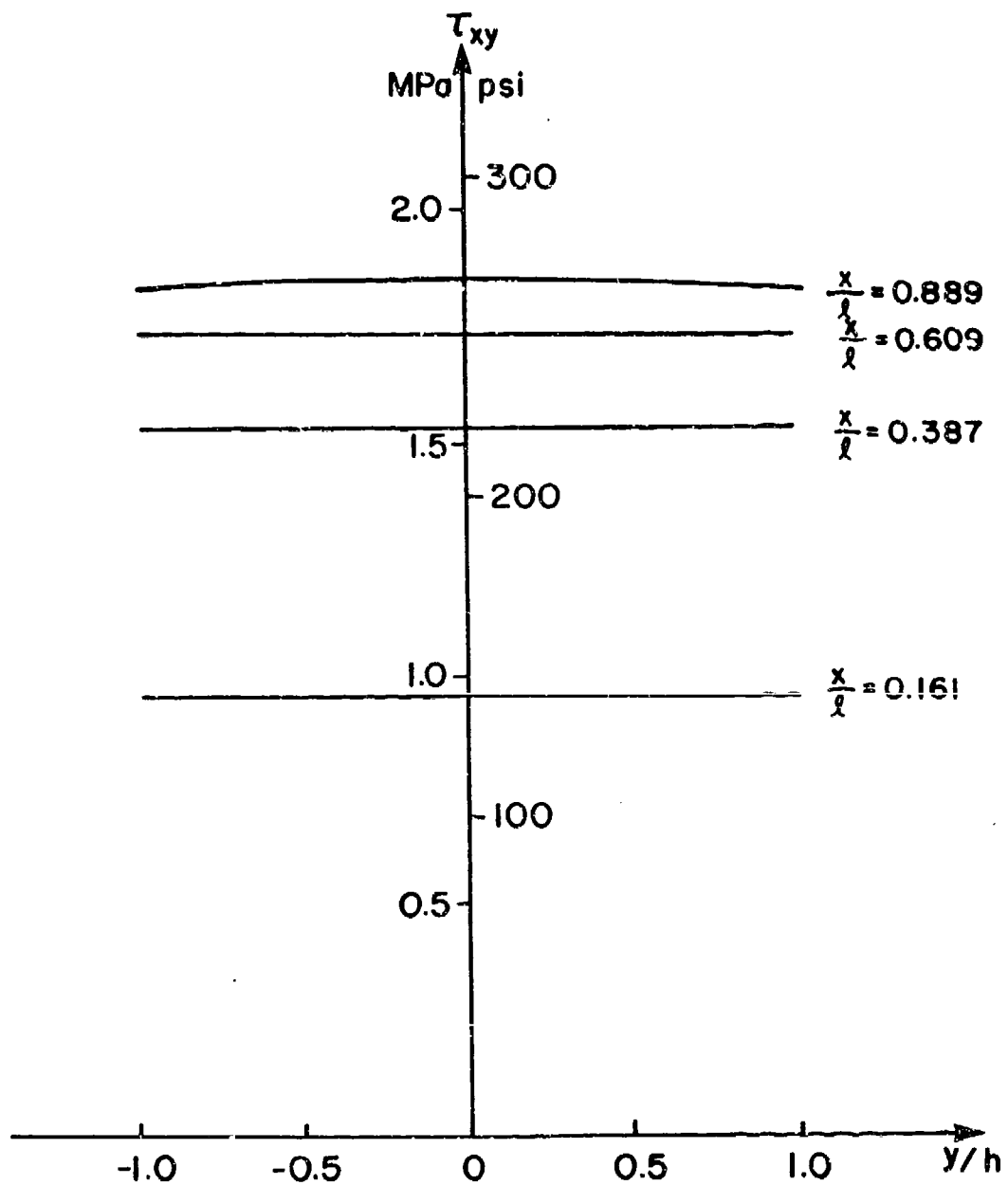


Figure 28. Variation of shear stresses over the thickness of the adhesive layer for various positions along the x-axis.

A limited numerical parametric study of the maximum shear stress in the adhesive layer is also conducted. Because of the numerical problem near the end of the beam, the values  $\tau_{xy}^{\max}$  -fin.el., as they are given in Table 2, are obtained by extrapolation of the undisturbed shear stress curves. Divided by  $P/bh$ , these maximum shear stresses can be compared to those obtained by the theoretical solution, for example by superposing them on Figure 31, resulting in Figure 29. Again, very good agreement between numerical and theoretical values is noted.

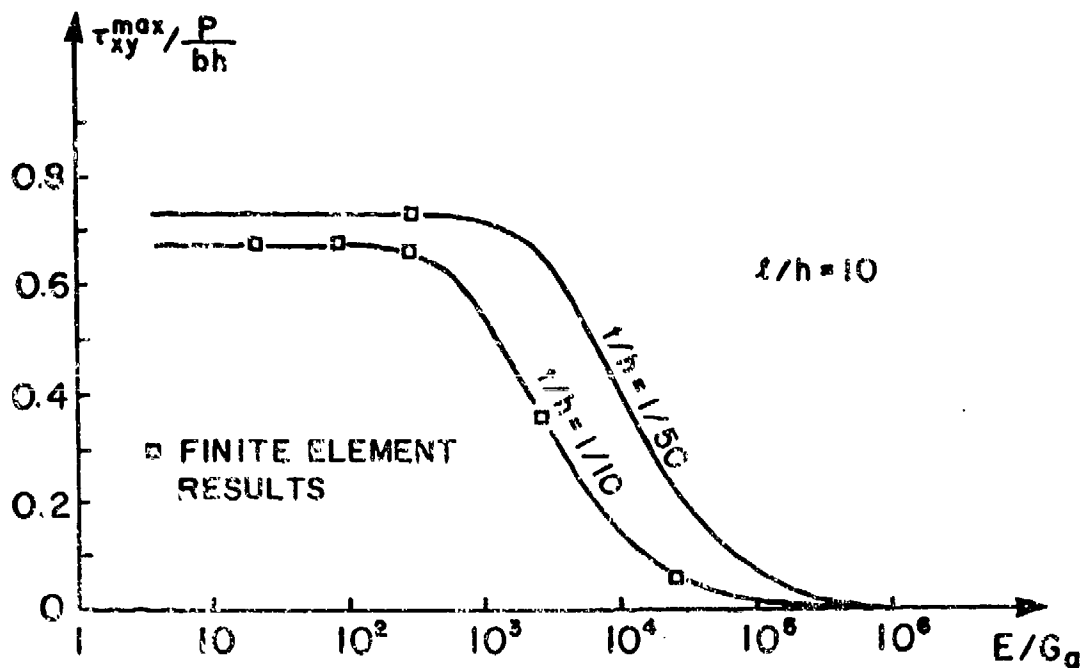


Figure 29. Comparison of numerically and theoretically obtained maximum shear stress values in the adhesive layer.

It can thus be concluded that the shear stress distribution in the adhesive layer can accurately be described by its strength-of-materials solution.

### 4.3 Effect of the Loading Mode

In Chapter 2, the load was assumed to be applied half at the upper adherend, half at the lower, for reasons of symmetry and to avoid introducing additional normal stresses in the adhesive layer. When the beam is loaded so that it moves downwards, compressive stresses will develop in the adhesive layer if the load is applied at the upper adherend, and will develop in the tensile stresses if the load is applied at the lower adherend (Figure 30).

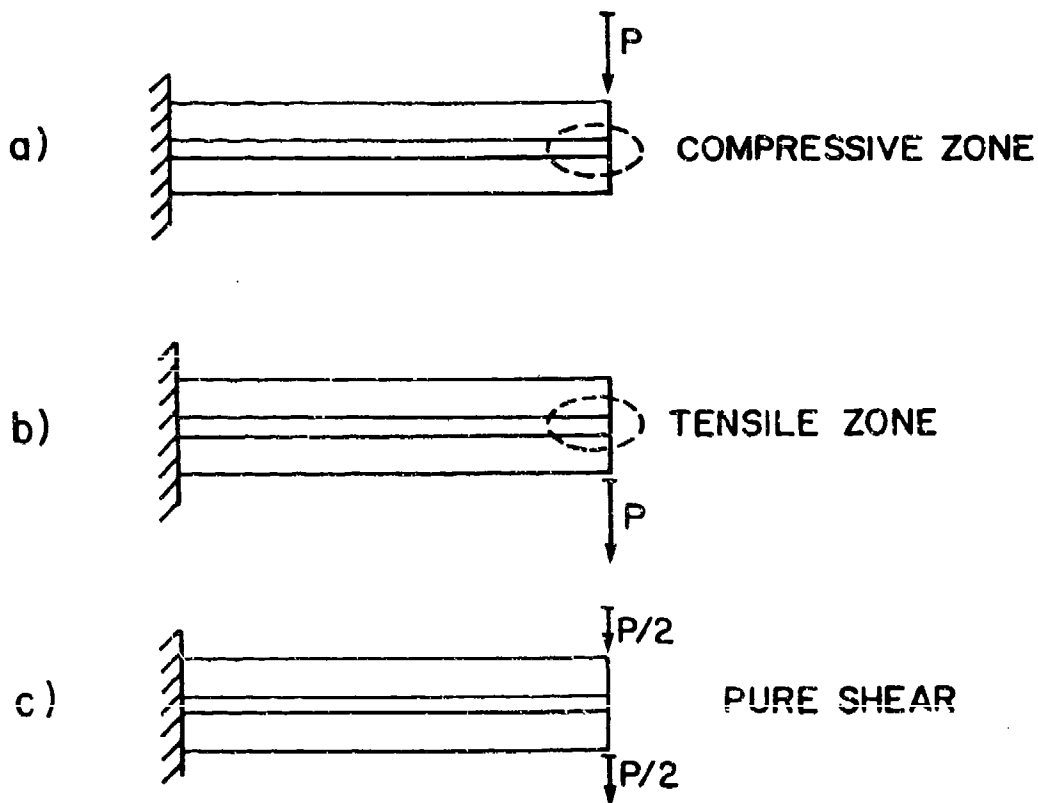


Figure 30. Effect of loading mode.

The stresses in the adhesive layer for a cantilever loaded at the lower adherend (Figure 30b) are numerically obtained and compared to the stresses for a beam equally loaded at the upper and lower adherend (Figure 31). The shear stress distributions for both cases are perfectly equal, whereas large normal stresses occur in the case of one-sided loading, compared to no normal stresses at all

for the other. This normal stress distribution is very similar to the one obtained near the ends of the overlap in lap joints, where these large tensile stresses are called peel stresses.

Because of the linearity assumption, the normal stresses in Figure 31 change signs only when the cantilever is loaded at the upper adherend and large compressive stresses are induced. As a matter of fact, the stresses as shown in Figure 31 are those that are obtained, except for the sign of the normal stresses  $\sigma_y$ , at the supported ends of a beam in three-point bending. In the middle of such a beam, where the load is applied, an additional compressive zone exists.

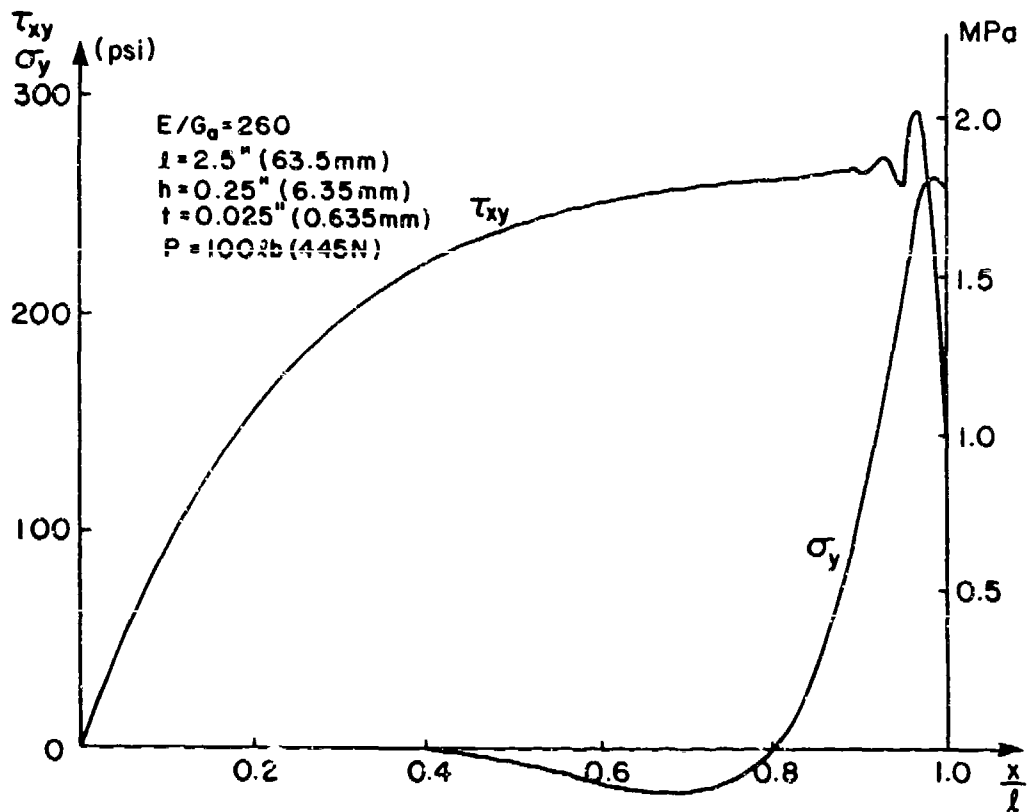


Figure 31. Shear stresses and normal vertical stresses in the adhesive layer for one-sided loading.

#### 4.4 Deflection of the Beam

The end deflections obtained by finite element analysis are compared to the theoretical values in Table 2 and Figure 32. Rather large differences are hereby noted, the theoretically obtained deflections being systematically 8 to 10 percent larger than the numerical ones. The reason the numerically obtained deflections are smaller is that they are computed for a plane strain assumption whereas Euler-Bernoulli beam theory is based on a plane stress situation, an option which is not provided in vista. A plane strain situation is found in bending of plates where transversal effects increase the bending stiffness by a factor  $1/(1-\nu^2)$  (13, pp. 288-290). For metals this increase means that the bending stiffness in the case of plane strain will be about 10 percent larger than for a plane stress case, which increase accounts for the 10 percent difference that was noticed between numerical and theoretical values.

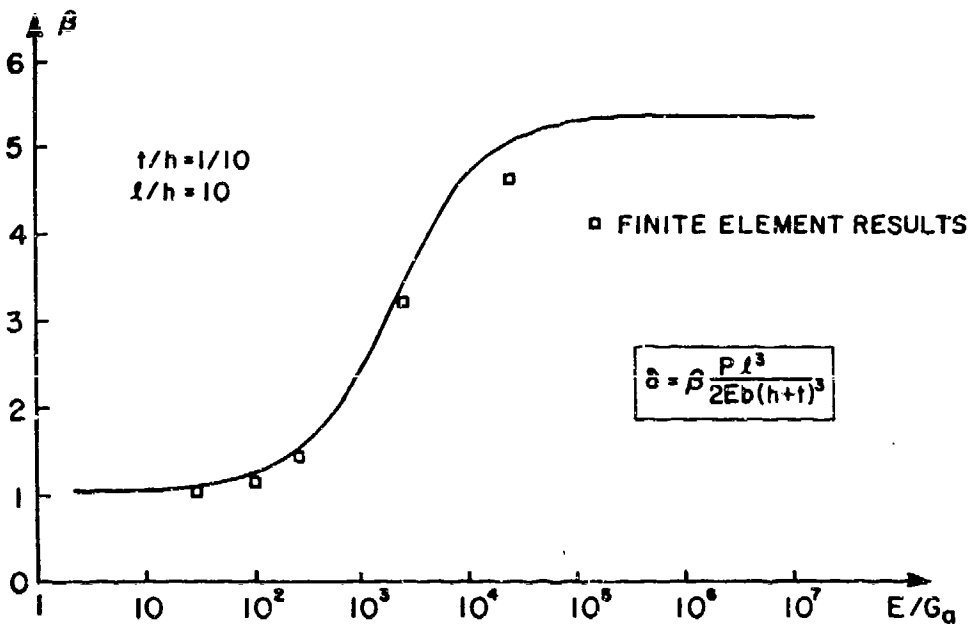


Figure 32. Comparison of the end deflection of the beam obtained by finite element analysis and by the strength-of-materials solution.

In Figure 33 the vertical displacements of the cantilever as obtained from finite element analysis and from the strength-of-materials solution are shown. In Figures 34 and 35, the deflections are depicted for two typical metal-adhesive combinations: steel adherends bonded by a rubber adhesive and aluminum adherends bonded by an epoxy adhesive, respectively used in the automotive and aerospace industries. They are compared to the deflections in the cases of "no adhesion" and "perfect adhesion." It is seen that for the rubber-steel beam, because of the very deformable adhesive layer, a very thin layer of the beam already leads to a large difference in the case of perfect adhesion, in contrast to the epoxy-aluminum beam where a third adhesive layer is necessary to obtain some sensitivity of the deflection to the presence of the adhesive layer.

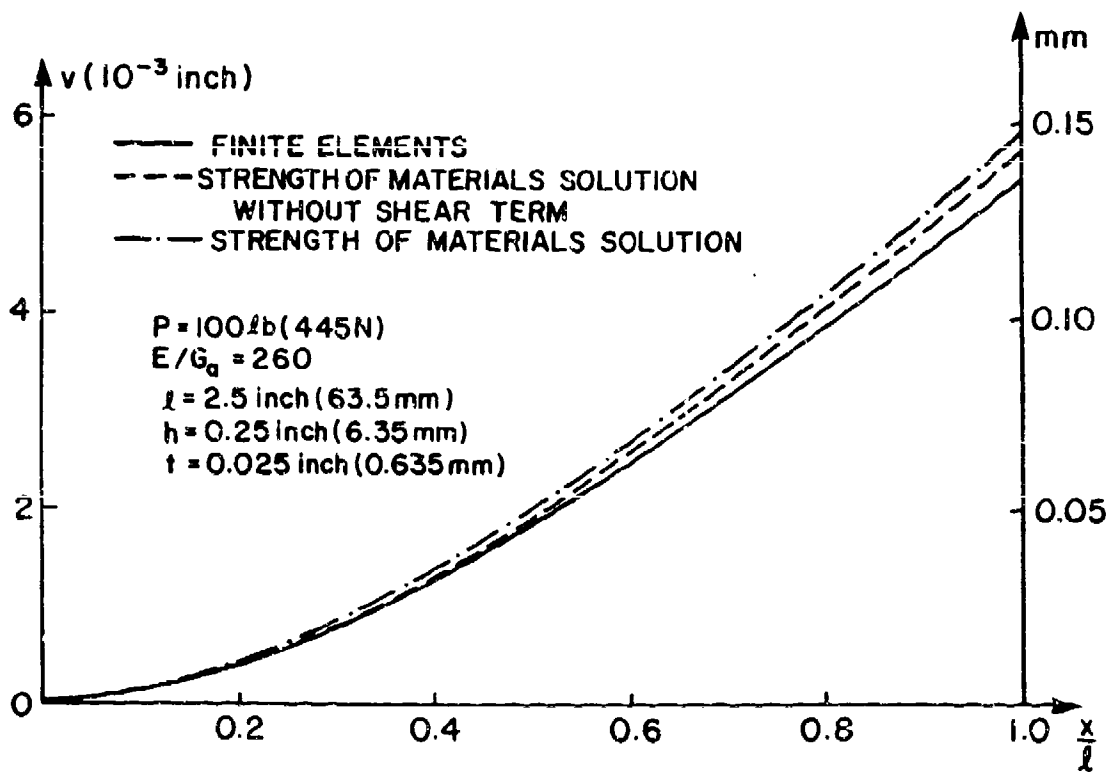


Figure 33. Comparison of the deflection of the cantilever beam obtained by finite elements and by the strength-of-materials solution.

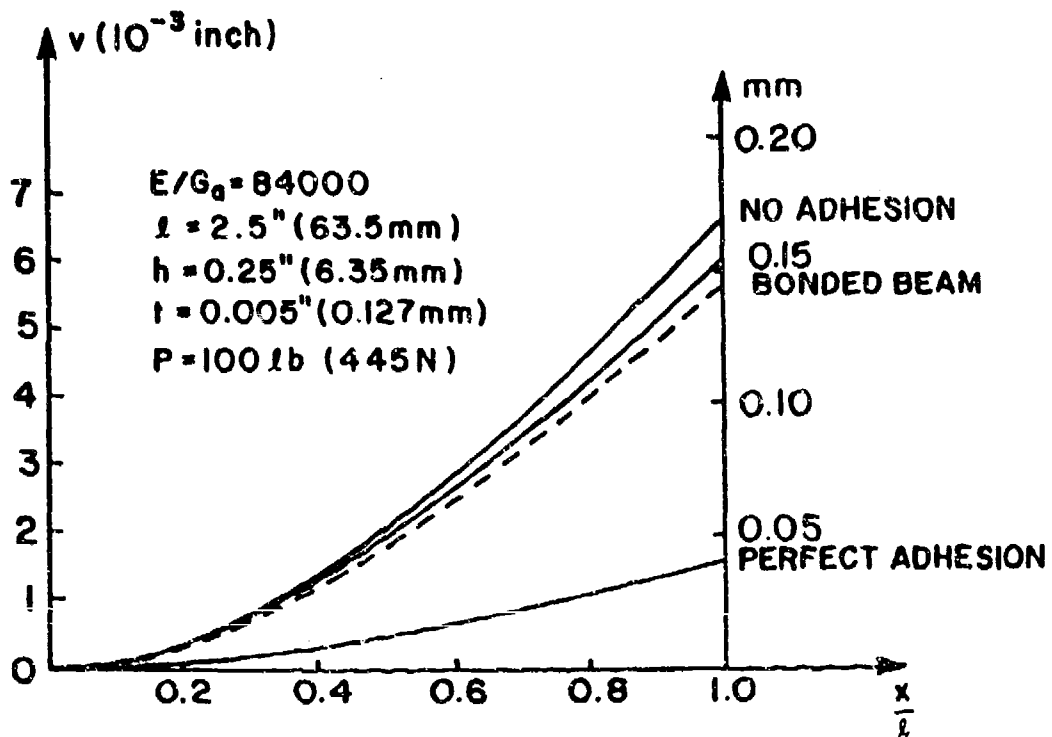


Figure 34. Deflection of a steel-rubber beam, compared to the cases of "perfect adhesion" and "no adhesion": ( $E = 30 \text{ msi } (207 \text{ GPa})$ ,  $G_a = 357 \text{ psi } (2.46 \text{ MPa})$ ); plane lines: theoretical values; slashed line: finite element values).

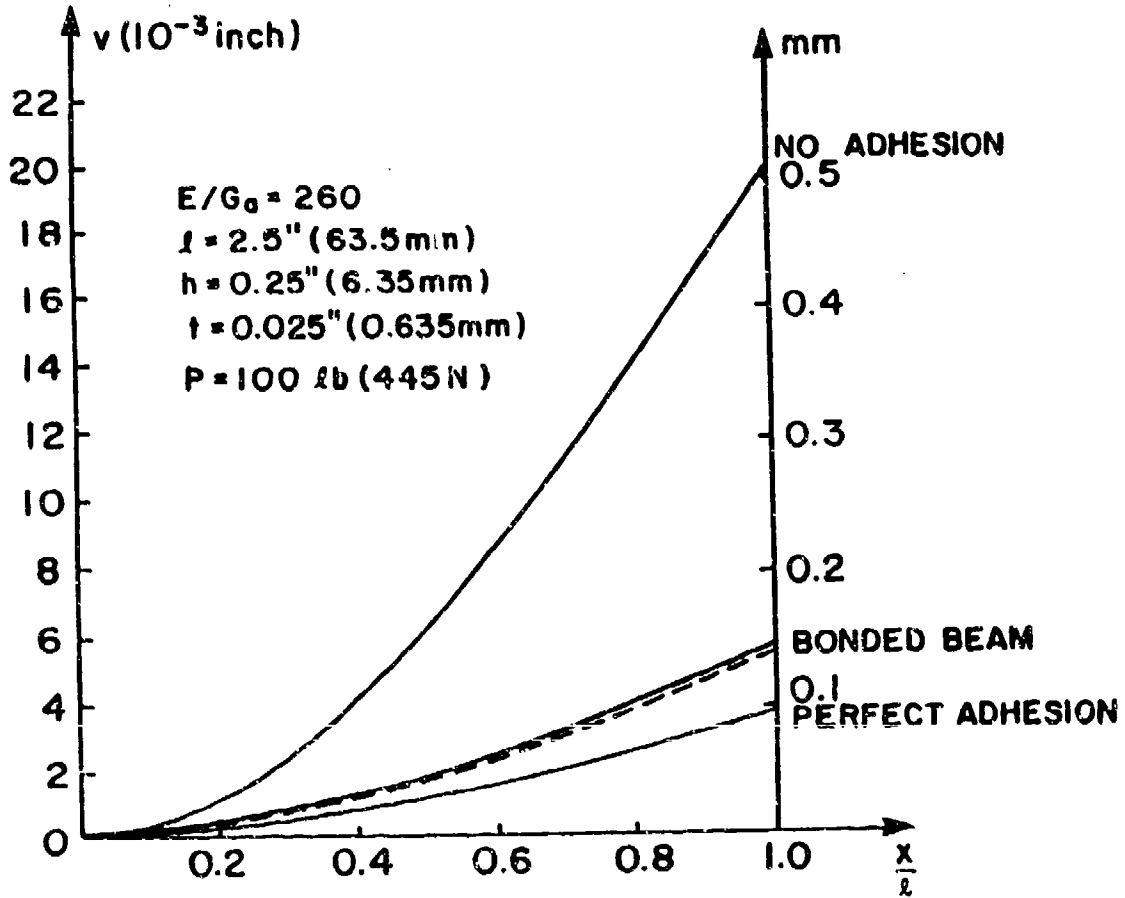


Figure 35. Deflection of an aluminum-epoxy beam, compared to the cases of "perfect adhesion" and "no adhesion": ( $E = 10 \text{ msi} (69 \text{ GPa})$ ,  $G_a = 38.5 \text{ ksi} (0.265 \text{ GPa})$ ; plane lines: theoretical values; slashed line: finite element values).

#### 4.5 Conclusions

From this numerical analysis three major conclusions can be drawn. The first is that the adhesive layer behaves indeed in a state of pure shear when the beam is equally loaded at both adherends, and that large normal stresses are induced in the adhesive layer near the loaded end when the beam is not so loaded. Second, there is excellent agreement for the shear stress distribution in the adhesive layer between numerical and theoretical results. And finally, although large differences

were noted for the deflection values, the agreement between theoretical and numerical results is fairly good considering the latter are based on a plane strain instead of a plane stress assumption.

## 5.0 RECOMMENDATIONS FOR FUTURE WORK

### 5.1 Introduction

Some ideas are presented in this chapter on how nonlinear elastic or viscoelastic behavior can be built into the strength-of-materials solution. Both material characteristics are in principle easily accounted for, but lead analytically to huge problems.

Also a possible use of the bended cantilever in the field of fracture mechanics is mentioned.

### 5.2 Nonlinear Adhesive Behavior

In the strength-of-materials solution of Chapter 2, adhesive behavior was introduced only in the continuity equation [2.12]. A linear elastic shear characteristic for the adhesive layer was assumed there, replacing the shear strain  $\gamma_{xy}$  in the adhesive by,

$$\gamma_{xy} = \frac{\tau_{xy}}{G_a} \quad [2.6]$$

The same deflection equation [2.4] and continuity equation [2.12] will be the starting point in this section, except that the shear strain in the adhesive will be induced as some nonlinear function of the shear stress,

$$EI \frac{d^2v}{dx^2} = \frac{P}{2} (\ell - x) - b \frac{h + 2t}{2} \int_x^\ell \tau_{xy}(\eta) d\eta \quad [2.4]$$

$$(h + 2t) \frac{dv}{dx} - 2t \gamma_{xy}(\tau_{xy}) - \frac{2}{Eh} \int_0^x \int_\eta^\ell \tau_{xy}(\lambda) d\lambda d\eta = 0 \quad [5.1]$$

In exactly the same way as in Chapter 2, the differential equation will be derived for  $\tau_{xy}$ : first by double differentiation of the continuity equation, then by single differentiation of the deflection equation, and finally by combining both resulting equations.

Double derivation of the continuity equation with respect to  $x$ ,

$$(h + 2t) \frac{d^3 v}{dx^3} - 2t \frac{d^2 \gamma_{xy}(\tau_{xy})}{dx^2} + \frac{2}{Eh} \tau_{xy}(x) = 0 \quad [5.2]$$

Derivation of the deflection equation with respect to  $x$ ,

$$EI \frac{d^3 v}{dx^3} = -\frac{P}{2} + b \frac{h + 2t}{2} \tau_{xy} \quad [5.3]$$

Elimination of the deflection term out of equations [5.2] and [5.3] and some rearrangement leads to the differential equation in  $\tau_{xy}$  and  $\gamma_{xy}$ ,

$$\frac{d^2 \gamma_{xy}(\tau_{xy})}{dx^2} - \left[ \frac{b(h + 2t)^2}{4tEI} + \frac{1}{Eht} \right] \tau_{xy}(x) = -\frac{P(h + 2t)}{4tEI} \quad [5.4]$$

This equation is identical to the one obtained for linear elastic behavior except for the first term which contains all the difficulty, since  $\gamma_{xy}$  is an implicit function of  $x$ . Using some advanced calculus theorems, we can develop that term,

$$\frac{d}{dx} \gamma_{xy} = \frac{\partial \gamma_{xy}}{\partial \tau_{xy}} \frac{d\tau_{xy}}{dx} \quad [5.5]$$

$$\frac{d^2}{dx^2} \gamma_{xy} = \frac{d}{dx} \left[ \frac{\partial \gamma_{xy}}{\partial \tau_{xy}} \frac{d\tau_{xy}}{dx} \right] = \frac{\partial \gamma_{xy}}{\partial \tau_{xy}} \frac{d^2 \tau_{xy}}{dx^2} + \frac{\partial^2 \gamma_{xy}}{\partial \tau_{xy}^2} \left[ \frac{d\tau_{xy}}{dx} \right]^2 \quad [5.6]$$

These equations finally lead to a nonlinear second order differential equation with varying coefficients. No analytical solutions exist for that kind of differential equation so that an exact solution can only be obtained by numerical means.

$$\frac{\partial \gamma_{xy}}{\partial \tau_{xy}} \frac{d^2 \tau_{xy}}{dx^2} + \frac{\partial^2 \gamma_{xy}}{\partial \tau_{xy}} \left[ \frac{d\tau_{xy}}{dx} \right]^2 - \left[ \frac{b(h+2t)^2}{4tEI} + \frac{1}{Eht} \right] \tau_{xy}(x) = - \frac{P(h+2t)}{4tEI} \quad [5.7]$$

A frequently used nonlinear characteristic is the power law, usually expressing  $\gamma_{xy}$  as a power function of  $\tau_{xy}$ . Considering the form of equation [5.7], the inverse relation will be used here, expressing  $\gamma_{xy}$  as a power function of  $\tau_{xy}$ , (equation [5.8]), although it is possible, but laborious, to express the differential equation in terms of  $\gamma_{xy}$ .  $k$ ,  $\ell$  and  $n$  are material constants.

$$\gamma_{xy} = k \tau_{xy} + \ell \tau_{xy}^n \quad [5.8]$$

$$\rightarrow \frac{\partial \gamma_{xy}}{\partial \tau_{xy}} = k + \ell n \tau_{xy}^{n-1} \quad [5.9]$$

$$\rightarrow \frac{\partial^2 \gamma_{xy}}{\partial \tau_{xy}^2} = \ell n(n-1) \tau_{xy}^{n-2} \quad [5.10]$$

Eventually the differential equation for the shear stress in the adhesive in the case of a power-law-material-behavior is obtained.

$$\left( k + \ell n \tau_{xy}^{n-1} \right) \frac{d^2 \tau_{xy}}{dx^2} + \ell n(n-1) \tau_{xy}^{n-2} \left[ \frac{d\tau_{xy}}{dx} \right]^2 - \left[ \frac{b(h+2t)^2}{4tEI} + \frac{1}{Eht} \right] \tau_{xy} = - \frac{P(h+2t)}{4tEI} \quad [5.11]$$

### 5.3 Viscoelastic Material Behavior

The correspondence principle (15) for problems in which one of the constituent materials shows time-dependent behavior, and for which an analytical solution is available, is used in this section. Since the strength-of-materials solution is a linear one, the behavior is restricted to linear viscoelasticity.

In the strength-of-materials solution for the bonded cantilever subjected to an end load, the shear stress in the adhesive layer, the maximum shear stress and shear strain in the same layer, and

the end deflection of the beam were respectively given by equations [2.34], [2.41], [2.42] and [2.53]. These equations are repeated here. The adhesive behavior was contained in parameter  $\bar{\alpha}$  only (equation [2.2i]).

$$\tau_{xy}(\xi) = \frac{P}{b\gamma^2(h+2t)} (1 - \cosh \bar{\alpha}\xi + \tanh \bar{\alpha} \sinh \bar{\alpha}\xi) \quad [2.34]$$

$$\tau_{xy}^{\max} = \frac{P}{b\gamma^2(h+2t)} \left[ 1 - \frac{1}{\cosh \bar{\alpha}} \right] \quad [2.41]$$

$$\gamma_{xy}^{\max} = \frac{P}{G_a b \gamma^2 (h+2t)} \left[ 1 - \frac{1}{\cosh \bar{\alpha}} \right] \quad [2.42]$$

$$\delta = \frac{P}{2Ebh^3} \left[ 4 \left( 1 - \frac{1}{\gamma^2} \right) + \frac{3E}{2G} \left( \frac{h}{\ell} \right)^2 + \frac{12}{\gamma^2} \left( \frac{1}{\bar{\alpha}} - \frac{\tanh \alpha}{\bar{\alpha}^3} \right) \right] \quad [2.53]$$

in which,

$$\gamma^2 = 1 + \frac{1}{3(1+2t/h)^2} \quad [2.20]$$

$$\bar{\alpha} = \gamma \sqrt{3 \frac{G_a}{E} \left[ \frac{\ell}{h} \right]^2 \frac{(1+2t/h)^2}{t/h}} \quad [2.21]$$

According to the correspondence principle, all time-dependent quantities have to be replaced by their Laplace transforms,  $s$  being the Laplace parameter.

$$P \rightarrow \bar{P}(s) \quad [5.12a]$$

$$G_a \rightarrow \bar{g}_a(s) \quad [5.12b]$$

$$\bar{\alpha} \rightarrow \bar{\alpha}(s) = \gamma \sqrt{3 \frac{\bar{g}_a(s)}{E} \left[ \frac{\ell}{h} \right]^2 \frac{(1+2t/h)^2}{t/h}} \quad [5.12c]$$

This leads - for example, for the maximum shear stress - to,

$$\bar{\gamma}_{xy}^{\max}(s) = \frac{\bar{P}(s)}{\bar{g}_a(s) b \gamma^2 (h+2t)} \left[ 1 - \frac{1}{\cosh \bar{\alpha}(s)} \right] \quad [5.13]$$

Then, the Laplace transforms have to be written in their explicit forms, assuming some viscoelastic model, Kelvin or Maxwell behavior for example, and some specific type of loading (creep loading, for example) (Figure 36).

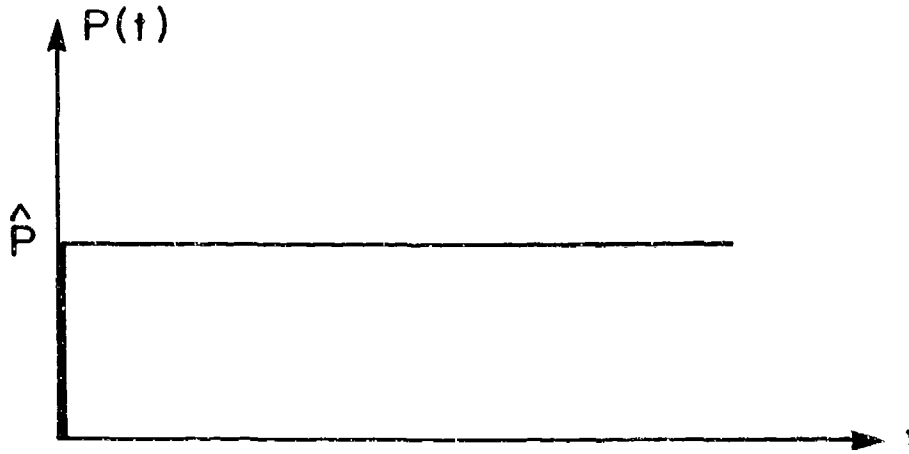


Figure 36. Creep loading.

---

For a creep test,

$$\bar{P}(s) = \frac{\hat{P}}{s} \quad [5.14]$$

Finally, to return to the time domain, the inverse Laplace transform of the equation under consideration needs to be taken, a procedure that, for the present problem, is easier said than done.

#### 5.4 Fracture Mechanics Application

The Double Cantilever Beam or DCB test is a known fracture test for adhesives (16). In this test the adherends in a bonded cantilever are pulled away from each other so that a crack in the adhesive layer will propagate in mode I (Figure 37).

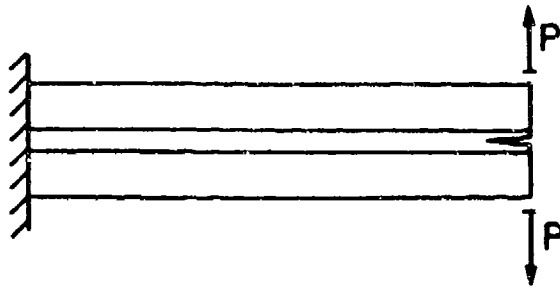


Figure 37. Double cantilever beam test.

---

In the case of a bonded cantilever beam loaded at the end by two equal forces in the same direction, the adhesive is now known to be in a state of pure shear, for which a solution is available. A crack in the adhesive layer will thus propagate in Mode II, so that this test geometry (Figure 38) can be used to obtain Mode II fracture energies.

---

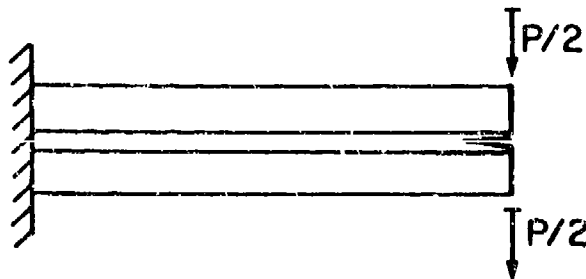


Figure 38. Bonded cantilever subjected to an end load.

---

Moreover, by making the end loads unequal, a mixed mode that can be seen as a superposition of modes I and II is obtained (Figure 39).

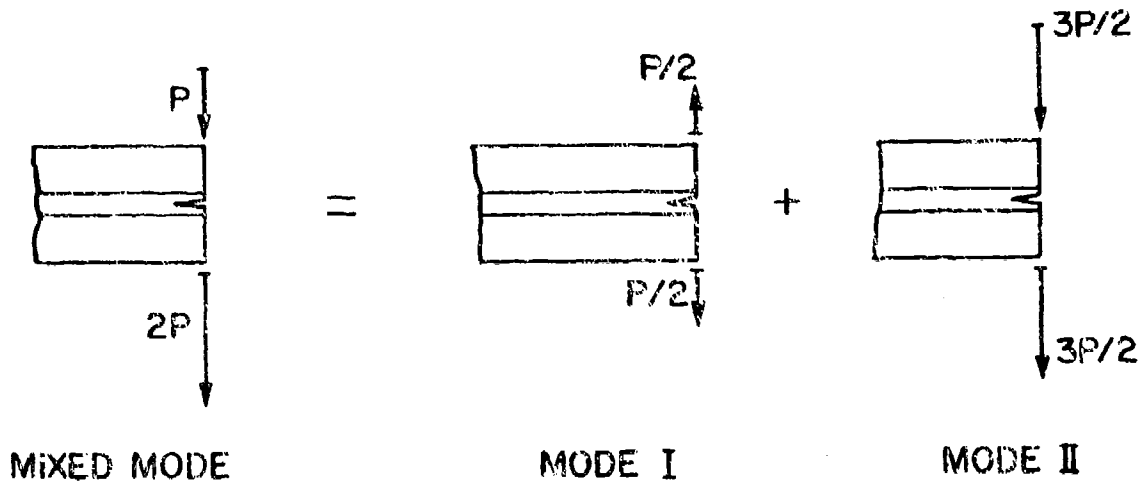


Figure 39. Bonded cantilever beam in mixed mode loading.

## 5.5 Conclusions

Introduction of nonlinear adhesive behavior in the strength-of-materials analysis leads to a nonlinear, second order differential equation with varying coefficients in the shear stress in the adhesive layer, for which no analytical solution exists. Numerical analysis is thus necessary for the case of nonlinear adhesive behavior.

Application of the superposition principle for linear viscoelastic adhesive behavior results in equations in the Laplace domain that are very difficult to transform to the time-domain.

The cantilever beam subjected to an end load can be used to obtain Mode II fracture characteristics and can be combined with the DCB Test to obtain mixed mode loading.

## 6.0 CONCLUSIONS

Use of a bonded cantilever beam specimen for the measurement of adhesive shear properties has been investigated. A strength of materials type solution is obtained for the shear stress state in the adhesive layer, sharing good agreement with finite element results.

Governed by the relative displacement of the adherends on both sides of the adhesive layer, the shear stress is shown to vary from zero at the fixed end to a maximum value at the free end. For relatively long beams and thin adhesive layers, a constant shear zone exists in the neighborhood of the free end. Under those conditions, that maximum shear stress can be calculated from a knowledge of the load and the beam geometry only. Therefore, by measuring the relative displacement between the adherends or the shear strain in the adhesive layer, the shear modulus can be determined. Numerically the shear stress is shown to be uniform through the thickness of the adhesive layer.

An expression for the beam deflection was obtained and related to the adhesive's shear modulus. A graphical method is presented to determine the modulus from deflection measurements. These deflection tests are also a simple way to compare surface treatments or different types of adhesives. To that purpose a coefficient of adhesion is introduced. For good sensitivity, relatively long beams and thick adhesive layers are recommended.

With the adhesive layer acting in a state of pure shear, the cantilever beam specimen can be useful to obtain mode II fracture energies. Implementation of nonlinear and viscoelastic adhesive behavior into the strength-of-materials solution is briefly mentioned.

## 7.0 References

1. ASTM Standards. "ASTM Test Method for Apparent Interlaminar Shear Strength of Parallel Fiber Composites by Short-Beam Method." Annual Board of ASTM Standards (1981-1984), ASTM D 2344.
2. Whitney, J. M., Browning, C. E., Mair, A. "Analysis of the Flexure Test for Laminated Composite Materials," *Composite Materials: Testing and Design*, ASTM 546, 1974, pp. 30-45.
3. Whitney, J. M., Browning, C. E. "On Short-Beam Shear Tests for Composite Materials," *Experimental Mechanics*, Vol. 25, No. 3, September 1985, pp. 294-300.
4. Browning, C. E., Abrams, F. L., Whitney, J. M. "A Four-Point Shear Test for Graphite-Epoxy Composites," ASTM STP 797.
5. Stinchcomb, W. W., Henneke, E. G., Price, H. L. "Use of the Short Beam Shear Test for Quality Control of Graphite-Polyimide Laminates," ASTM STP 626, 1977, pp. 96-109.
6. Sattar, S. A., Kellogg, D. H. "The Effect of Geometry on the Mode of Failure of Composites in Short Beam Shear Tests," *Composite Materials: Testing and Design*, ASTM STP 460, 1969, pp. 62-71.
7. Kedward, K. T. "On the Short Beam Method," *Fiber Science and Technology*, Vol. 5, 1972, pp. 85-95.
8. Berg, C. A., Tirosh, J., Israeli, M. "Analysis of Short Beam Bending of Fiber Reinforced Composites," ASTM STP 497.
9. Sandoff, P.E. "St. Venant Effects in an Orthotropic Beam," *Journal of Composite Materials*, Vol. 14, July 1980, pp. 199-212.
10. Abdallah, M. G. "Review of the State-of-the-Art of Advanced Composite Interlaminar Shear Stress Methods," Hercules, Testing and Methods Development MS 2343A, EXT 23539.
11. Peters, P. W. M. "The Interlaminar Shear Strength of Unidirectional Boron-Aluminum Composites," *Journal of Composite Materials*, Vol. 12, January 1978, pp. 53-62.
12. Beck, H. "Contributions to the Analysis of Coupled Shear Walls," *ACI Journals*, August 1962, pp. 1055-1069.
13. Timoshenko, S. P., Goodier, J. N. *Theory of Elasticity*. McGraw-Hill.
14. Timoshenko, S. P. *Strength of Materials. Part I: Elementary Theory and Problems*, Van Nostrand Reinhold.
15. Christensen, R. M. *Theory of Viscoelasticity: An Introduction*, Academic Press, 1971.
16. Anderson, G. P., Bennett, S. J., DeVries, K. L. *Analysis and Testing of Adhesive Bonds*, Academic Press, 1977.

BIBLIOGRAPHIC DATA SHEET		1. Report No. VPI-E-87-9	2.	3. Recipient's Accession No.
4. Title and Subtitle CAS/ESM-87-2 BENDING OF A BONDED BEAM AS A TEST METHOD FOR ADHESIVE PROPERTIES			5. Report Date	
7. Author(s) Moussiaux, E., Brinson, H. F., Cardon, A. H.			6.	
9. Performing Organization Name and Address Virginia Polytechnic Institute & State University Department of Engineering Science and Mechanics Center for Adhesion Science Blacksburg, VA 24061			8. Performing Organization Rept. No.	
12. Sponsoring Organization Name and Address Office of Naval Research Code 431 800 N. Quincy Street Arlington, VA 22217			10. Project/Task/Work Unit No.	
			11. Contract/Grant No. N00014-82-K-0185	
			13. Type of Report & Period Covered Sept 86 - June 87	
15. Supplementary Notes			14.	
16. Abstracts <p>A strength-of-materials type solution is obtained for the shear stress state in the adhesive layer of a bonded cantilever beam subjected to an end load.</p> <p>The shear stress is constant through the thickness of the adhesive layer and varies from zero at the fixed end to a maximum value at the free end. This maximum value can, under certain conditions, be calculated from knowledge of the load and the beam geometry only. The adhesive's shear modulus can then be determined from a measurement of the shear strain in the adhesive layer.</p> <p>An expression for the beam deflection is also obtained. It contains a coefficient of adhesion which is potentially useful in evaluating surface treatments or other factors leading to different states of adhesion.</p> <p>Fracture mechanics application of the specimen, and nonlinear and viscoelastic adhesive behavior are briefly mentioned.</p>				
17. Key Words and Document Analysis. 17a. Descriptors <p>Bonded beam, test specimen, adhesive shear modulus, finite element analysis, nonlinear elasticity, viscoelasticity</p>				
17b. Identifiers/Open-Ended Terms				
17c. COSATI Field/Group				
18. Availability Statement Distribution unlimited			19. Security Class (This Report) UNCLASSIFIED	21. No. of Pages 82
			20. Security Class (This Page) UNCLASSIFIED	22. Price